

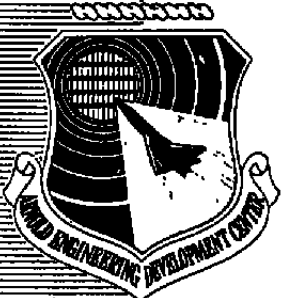
UNCLASSIFIED

DEC 2 1975

AEDC-TR-75-49

cy.2

DOC_NUM	SER	CN
UNC11297-PDC	A	1



A STUDY OF THE JETTISONING OF JP-4 FUEL IN THE ATMOSPHERE

VON KÁRMÁN GAS DYNAMICS FACILITY
ARNOLD ENGINEERING DEVELOPMENT CENTER
AIR FORCE SYSTEMS COMMAND
ARNOLD AIR FORCE STATION, TENNESSEE 37389

November 1975

Final Report for Period July 1, 1972 — August 31, 1974

Approved for public release; distribution unlimited.

Prepared for

AIR FORCE CIVIL ENGINEERING CENTER (EVA)
KIRTLAND AFB, NEW MEXICO 87117

Property of U. S. Air Force
AEDC LIBRARY
F40600-75-C-0001

UNCLASSIFIED

NOTICES

When U. S. Government drawings specifications, or other data are used for any purpose other than a definitely related Government procurement operation, the Government thereby incurs no responsibility nor any obligation whatsoever, and the fact that the Government may have formulated, furnished, or in any way supplied the said drawings, specifications, or other data, is not to be regarded by implication or otherwise, or in any manner licensing the holder or any other person or corporation, or conveying any rights or permission to manufacture, use, or sell any patented invention that may in any way be related thereto.

Qualified users may obtain copies of this report from the Defense Documentation Center.

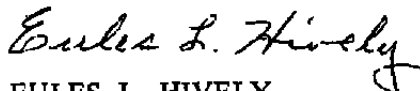
References to named commercial products in this report are not to be considered in any sense as an endorsement of the product by the United States Air Force or the Government.

This report has been reviewed by the Information Office (OI) and is releasable to the National Technical Information Service (NTIS). At NTIS, it will be available to the general public, including foreign nations.

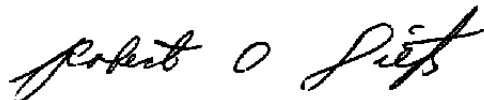
APPROVAL STATEMENT

This technical report has been reviewed and is approved for publication.

FOR THE COMMANDER



EULES L. HIVELY
Research & Development
Division
Directorate of Technology



ROBERT O. DIETZ
Director of Technology

UNCLASSIFIED

REPORT DOCUMENTATION PAGE		READ INSTRUCTIONS BEFORE COMPLETING FORM
1 REPORT NUMBER AEDC-TR-75-49	2 GOVT ACCESSION NO.	3 RECIPIENT'S CATALOG NUMBER
4 TITLE (and Subtitle) A STUDY OF THE JETTISONING OF JP-4 FUEL IN THE ATMOSPHERE		5 TYPE OF REPORT & PERIOD COVERED Final Report - July 1, 1972 - August 31, 1974
		6 PERFORMING ORG REPORT NUMBER
7 AUTHOR(s) R. Dawbarn, K. W. Nutt, and C. W. Pender, ARO, Inc.		8 CONTRACT OR GRANT NUMBER(s)
9 PERFORMING ORGANIZATION NAME AND ADDRESS Arnold Engineering Development Center (DY) Air Force Systems Command Arnold Air Force Station, Tennessee 37389		10 PROGRAM ELEMENT, PROJECT, TASK AREA & WORK UNIT NUMBERS Program Element 62601F Project 1900
11 CONTROLLING OFFICE NAME AND ADDRESS Arnold Engineering Development Center (DYFS) Arnold Air Force Station, Tennessee 37389		12 REPORT DATE November 1975
		13 NUMBER OF PAGES 81
14 MONITORING AGENCY NAME & ADDRESS (if different from Controlling Office)		15 SECURITY CLASS. (of this report) UNCLASSIFIED
		15a DECLASSIFICATION DOWNGRADING SCHEDULE N/A
16 DISTRIBUTION STATEMENT (of this Report) Approved for public release; distribution unlimited.		
17 DISTRIBUTION STATEMENT (of the abstract entered in Block 20, if different from Report)		
18 SUPPLEMENTARY NOTES Available in DDC		
19 KEY WORDS (Continue on reverse side if necessary and identify by block number) fuel jet engine fuels droplet evaporation drops JP-4 condensation liquids air pollution hydrocarbons particles droplet coalescence		
20 ABSTRACT (Continue on reverse side if necessary and identify by block number) This study was undertaken at AEDC to provide information relating to the impact on the environment when JP-4 fuel is jettisoned from jet planes. The specific areas investigated were (1) the physical breakup of the JP-4 into droplets, (2) the physical properties of JP-4, (3) the drag coefficient of JP-4 droplets, (4) the evaporation characteristics of JP-4 droplets, and (5) the effects of JP-4 on the atmospheric processes of condensation of water vapor. Data		

UNCLASSIFIED

UNCLASSIFIED

20. ABSTRACT Continued

and information provided in the first four areas should be useful in developing a computer model to predict the eventual distribution of JP-4 from a specific fuel dump under particular atmospheric conditions. The results of the studies in the area of atmospheric condensation indicate JP-4 vapors should have negligible effects. However, small JP-4 droplets may act as effective seed nuclei to initiate precipitation under favorable conditions.

UNCLASSIFIED

PREFACE

The work reported herein was sponsored by the Air Force Civil Engineering Center/EVA, formerly the Air Force Weapons Laboratories/DE, Kirtland AFB, New Mexico, under Program Element 62601F, Project No. 1900. The results presented were obtained by ARO, Inc. (a subsidiary of Sverdrup & Parcel and Associates, Inc.), contract operator of the Arnold Engineering Development Center (AEDC), Air Force Systems Command (AFSC), Arnold Air Force Station, Tennessee. This work was conducted under ARO Project No. VF460-13YA. The authors of this report were R. Dawbarn, K. W. Nutt, and C. W. Pender, ARO, Inc. The manuscript (ARO Control No. ARO-VKF-TR-74-107) was submitted for publication on November 4, 1974.

CONTENTS

	<u>Page</u>
1.0 INTRODUCTION	7
2.0 JETTISONING FROM AIRCRAFT AND BREAKUP OF LIQUID	10
3.0 PROPERTIES OF JP-4 FUEL	
3.1 Density	20
3.2 Vapor Pressure	22
3.3 Surface Tension	24
3.4 Latent Heat of Vaporization	26
3.5 Specific Heat	27
4.0 DROPLET BREAKUP AND COALESCENCE	
4.1 Breakup of Liquid Jet	29
4.2 Coalescence of Droplets	31
5.0 DRAG COEFFICIENT OF FREE-FALLING DROPLETS	
5.1 Experimental Apparatus	32
5.2 Results	34
5.3 Discussion	35
5.4 Application of Data to Atmospheric Tests	36
6.0 EVAPORATION OF JP-4 DROPLETS	
6.1 Experimental Apparatus	40
6.2 Experimental Procedure	41
6.3 Analysis of Evaporated Components of JP-4	41
6.4 Calibration of the Gas Chromatograph	42
6.5 Discussion	47
7.0 EVAPORATION RATES OF JP-4 DROPLETS	
7.1 Experimental Apparatus	48
7.2 Experimental Procedure	52
7.3 Data Reduction	52
7.4 Results	56
8.0 VAPOR PRESSURE OF JP-4 AND RESIDUALS	
8.1 Experimental Apparatus	62
8.2 Experimental Procedure	63
8.3 Discussion	63
9.0 EFFECTS OF JP-4 ON CONDENSATION OF ATMOSPHERIC WATER VAPOR	
9.1 Experimental Apparatus	70
9.2 Experimental Procedure	71
9.3 Results	71
9.4 Discussion	74
10.0 SUMMARY OF RESULTS	75
REFERENCES	76

ILLUSTRATIONS

<u>Figure</u>	<u>Page</u>
1. Droplet Size Distribution from Fuel Dumping	11
2. Droplet Size as a Function of Liquid Jet Diameter. . .	15
3. Maximum Droplet Size as a Function of Relative Velocity	16
4. Critical Velocity for Droplet Breakup	17
5. Specific Gravity of JP-4 versus Temperature	22
6. Vapor Pressure of Various Hydrocarbons	24
7. Surface Tension as a Function of Temperature	25
8. Latent Heat of Vaporization of JP-4	26
9. Specific Heat as a Function of Temperature	27
10. Schematic of Drop Tube	32
11. Velocity Profile of Falling Water Droplet	34
12. Plots of Drag Coefficient versus Reynolds Number for Disks, Spheres (Solid and Liquid) and Water Droplets	34
13. Drag Coefficient versus Reynolds Number for JP-4 Droplets	35
14. Plot of Re versus $Re \sqrt{C_D}$ for JP-4	37
15. Plot of Re versus C_D/Re for JP-4	38
16. Schematic of Closed-Loop Wind Tunnel	40
17. Gas Chromatograms of JP-4 and Fractions	44
18. Gas Chromatograms of 1-ml Fractions	45
19. Typical Chromatograms of Evaporation Samples . . .	46
20. Pendant Drop Test Apparatus.	49
21. Drop Support and Adjustable Nozzle	50
22. JP-4 Droplet on Glass Filament	51
23. Evaporating Droplet on Sting	53

<u>Figure</u>	<u>Page</u>
24. Map of Suspended Droplet	54
25. Evaporation Rate as a Function of Time	56
26. Evaporation Rate of JP-4 Droplets	58
27. Evaporation Rate of JP-4 at Various Humidities . . .	59
28. Evaporation Rate of JP-4 for Various Air Velocities	59
29. Evaporation Rate versus Air Velocity	60
30. Evaporation of Droplets in Cooled Airflows	60
31. Evaporation Rate of JP-4 Fractions	61
32. Schematic of Apparatus Used to Measure Vapor Pressure	62
33. Vapor Pressure of JP-4 and Residuals	64
34. Schematic of Cloud Chamber	66
35. Critical Supersaturation as a Function of Particle Radius	69
36. Concentration of Condensation Nuclei in Atmosphere	69

TABLES

1. Properties of Defoliant	12
2. Specifications of JP-4	21
3. Droplet Data Produced from Spray Tests	29
4. Properties of JP-4 Fractions	42
5. Analysis of JP-4 Fractions	43
6. Empirically Determined Constants for Evaporation Rate Equation	61
7. Densitometer Readings	72
NOMENCLATURE	79

1.0 INTRODUCTION

Widespread public attention was first focused on the possible pollution problem caused by jet fuel being jettisoned in the atmosphere when a commercial airline pilot was fired for insubordination because he continued to demand that residual fuel in pressurization and dump fuel drain cans on his aircraft's jet engines be drained prior to take-off. This fuel (approximately 1 to 2 lb), which drains into the cans during engine start and shutdown, is automatically siphoned out of the cans by air pressure as the aircraft accelerates. The siphoning action is designed to start by ram air pressure when the aircraft reaches an indicated airspeed of approximately 200 knots. However, there is considerable disagreement over where the fuel is jettisoned and what happens to it. Some argue that the fuel is ejected at about 2000-ft altitude and about five miles from the runway. This view is countered by some pilots who are convinced that they have seen the fuel spill on the runway itself. Those who are convinced that the fuel is vented at altitude are divided in their opinion of what happens to the fuel after being released. The commercial airlines suggest that it is completely vaporized and so diluted by prevailing winds that it presents no significant pollution problem. National Air Pollution Control Authority (NAPCA) officials argue that kerosene does not vaporize quickly and that much of the discarded fuel remains as a fine aerosol suspended in the atmosphere presenting a localized pollution problem, especially in the air corridors used for takeoff from airports (Ref. 1).

In addition to the above-described routine operations, unusual conditions occur where the disposal of large quantities of fuel is necessary. These conditions exist with a wide range of latitude. In some cases, there are emergency conditions which necessitate the immediate off-loading of the fuel at as high a rate as possible. In other cases, even though they represent an emergency, there is some amount of control over the conditions of release. An incident at the San Francisco airport involving damage to a 747 during takeoff represented such a case. The situation with the most latitude is that where a flight must be aborted because of conditions which do not involve potential danger to lives. In such cases the conditions of release of the fuel, that is, the altitude, flight velocity, and rate of flow, may be completely open to the discretion of the pilot. At the present time, there is very little information available which can be used to evaluate the effects on the local environment caused by thousands of pounds of JP-4 fuel being sprayed into the atmosphere. Recommendations to release the fuel at high or

low altitude, to seek or avoid cloud layers, to reduce or increase air-speed, etc., cannot be made until the effects of these variables are known.

The conditions and potential impacts of the military and commercial fleets are essentially similar; the examples above serve equally well for either operation. The research and test programs described in this report were addressed to the particular problem of the jettisoning of JP-4 fuel into the atmosphere and its resulting impact on the environment.

Fuel jettisoned at altitude will break up into droplets as the liquid stream encounters the high-speed airstream. For a short period of time these droplets will be entrained in the turbulent wake of the aircraft and one can expect vapor from the fuel at this point to be thoroughly mixed with the exhaust products from the aircraft's engines. As the turbulent energy in the wake is dissipated, the droplets of fuel will start to free fall. During the early phases of free fall several processes may occur. Small droplets may coalesce thus forming larger drops, and extremely large droplets may break up due to the aerodynamic forces on them as they accelerate under gravitational forces. Thus, there may be a readjustment of the size distribution of the falling droplets. Throughout the falling process the droplets will be evaporating, leaving a hydrocarbon vapor in the atmosphere. It is possible that under the appropriate conditions (low-altitude dump, cold temperatures) some of the JP-4 may survive the free fall and cause a ground contamination problem.

The most publicized atmospheric pollution problem (smog) results from the reaction of hydrocarbon vapors and oxidants (Ref. 2). This reaction is triggered by the ultraviolet radiation present in sunlight. Obviously, the addition of a considerable quantity of hydrocarbons to the atmosphere should cause concern about the photochemical processes which may occur. The two areas possibly of most importance in this respect are (1) the aircraft wake, where there is sufficient concentration of oxidants from the jet engine exhausts and (2) at ground level in a metropolitan area where automobile exhausts supply the oxidants.

The work accomplished in this phase of the project does not pursue this aspect of the problem. However, data obtained in the evaporation studies may be useful in defining the class of hydrocarbons most likely to remain as vapors in the aircraft wake and in the ground level mixing layer.

A second area of concern can reasonably be voiced when considering the impact of JP-4 vapors on the atmospheric hydrological cycle. The normal atmospheric processes of cloud formation, rainfall, and subsequent evaporation provide a natural cycle which cleanses particulates from the atmosphere. The bulk of these particles are dusts from wind erosion and hygroscopic salts from evaporated salt water sprays. While these may be classified in an absolute sense as pollutants, they are a necessary part of the hydrological cycle. These small particles act as nucleation sites for aggregation of water molecules. Addition of JP-4 to the atmosphere may prove to be only a minor perturbation to the natural cycle and be effectively washed out in subsequent rainfalls. It is suspected, however, that the impact of the fuel jettison may have more far-reaching effects. It is well known that the more effective condensation nuclei are those which are classified as "wetttable", the hygroscopic salts being the most efficient. Contaminated by JP-4 fuel, these particles may become "nonwetttable" and thus incapable of serving as condensation nuclei. If this occurs, there will be an abnormal increase in the naturally occurring particulates, since the cleansing process due to precipitation as rain or ice will be inhibited.

Cloud and fog banks which at first seem to be quiescent, are, in fact, constantly involved in the process of condensation and evaporation. Water droplets which grow within the fog-cloud structure reach such a size that gravitational forces overcome the aerodynamic forces produced by updrafts, and they start to fall. However, as they leave the high humidity of the cloud layer, they re-evaporate and are swept back into the cloud to repeat this cycle. Addition of an unusual quantity of impurities could greatly affect this process. Evidence exists which suggests that some hydrocarbon concentrations, low enough to create a monolayer coverage on water droplets, can inhibit evaporation and thus stabilize fog and cloud formations to the point where they cannot dissipate by the natural methods of precipitation or evaporation (Ref. 3).

The experimental work reported herein was designed and conducted to answer questions which were raised as a result of a survey of pertinent literature. The subjects considered were as follows:

1. Direct references to jettisoning of liquids from aircraft and breakup of liquids in high-speed air streams;
2. Properties of JP-4;

3. Droplet fallout and evaporation --
 - a. coalescence of droplets,
 - b. drag coefficients,
 - c. evaporation rates; and
4. Effects of JP-4 vapor on condensation and evaporation of water vapor.

2.0 JETTISONING FROM AIRCRAFT AND BREAKUP OF LIQUID

There is surprisingly little information in the literature that is specifically addressed to the problem of dumping fuel from aircraft. Cross and Picknett report on low-altitude fuel dumps conducted at Porton Downs in August of 1972 (Ref. 4). The technique used was to fly across the wind at an altitude of approximately 15 meters and dump fuel to which had been added 0.5-percent Unitex SWN. Unitex SWN is highly fluorescent under ultraviolet radiation. The droplets were collected on filter papers located downwind, and the droplet sizes were determined by the quantity of Unitex SWN residual remaining on the filters. From these data the authors present a drop-size distribution curve and suggest an empirical equation for the mass median size,

$$d(\mu\text{m}) = 155 + (0.17 \pm 0.06)f$$

where f is the fuel flow rate in kg/min.

This equation would be applicable for an aircraft flying at 120 m/sec (234 knots) and dumping through a 6-cm (2.5-in.)-diam pipe. As can be seen from the curve in Fig. 1, the maximum droplet size from these tests was 400 μm with a mass median diameter of 240 μm . It is noted that in taking inventory of the total fuel dumped and the quantity observed at ground level that only 55 percent of the fuel could be accounted for. The authors suggest that shielding of sample collectors by tall grasses and a possible loss of some smaller particles due to evaporation as the most likely explanation. A second explanation is that much more of the fuel than the authors suspect is contained in droplets with diameters less than 50 μm . It is unfortunate that no information is presented as to the velocity of the crosswind during the test periods. Assuming, however, a relatively slight windspeed of 2.5 m/sec (5 knots), a 50- μm droplet

falling at its terminal velocity of approximately 7.6 cm/sec (0.24 ft/sec) would drift well beyond the far line of sample collectors, 350 m (1132 ft) during its 15-m (50-ft) free fall. It is also noted that the resolution of the detection technique did not permit observation of droplets smaller than 40 μm .

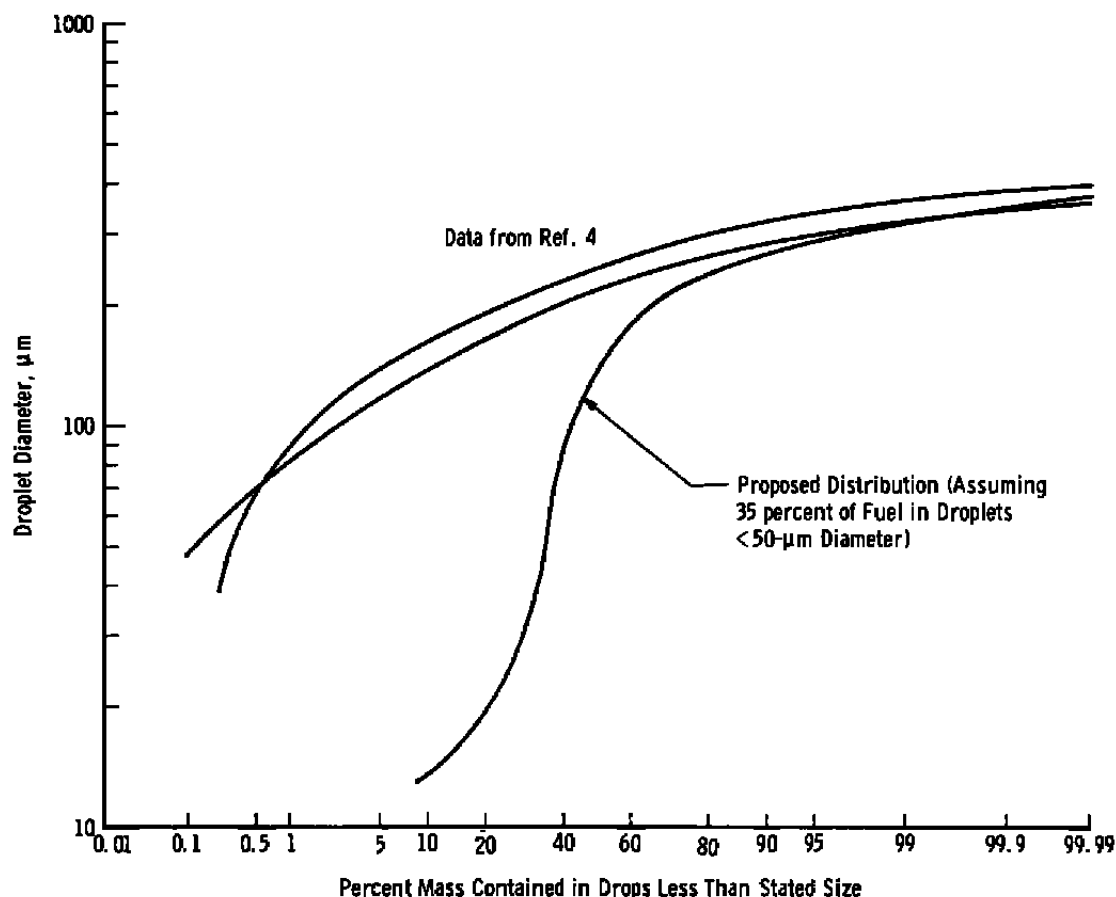


Figure 1. Droplet size distribution from fuel dumping.

Evidence to support the production of a significant number of smaller droplets is contained in test results obtained in wind tunnel tests conducted by Davidson (Ref. 5) and Wasson, et al. (Ref. 6). The former tests were conducted with simulated defoliant as the liquid, with dump rates of 14.5 to 558 kg/min (33 to 1280 lb/min) in a 205-m/sec (400-knot) airstream. A comparison of the defoliant's properties compared to JP-4 is given in Table 1.

Table 1. Properties of Defoliant

Property at 70°F	Defoliant	JP-4	H ₂ O
Specific gravity	1.34	0.77	1.00
Viscosity (centistokes)	8.80	1.60	1.00
Surface Tension (dyne/cm)	35.00	21.00	73.00

The results reported (Ref. 5) indicate that all the droplets detected were less than 50 μm in diameter with a mass median diameter of 24 μm .

Similarly the data produced by Wasson, et al. for JP-4 fuel indicate a maximum droplet size of 100 μm with mass median droplet sizes ranging from 25 to 55 μm . These tests involved flow rates of JP-4 fuel from 1.3 to 136 kg/min (13 to 300 lb/min).

Both investigators used an in-line holographic technique to record the droplets produced. In each case the photographic station was located relatively close to the dump nozzle because of the limitations imposed by the length of the test cell.

It is obvious that these results are not entirely consistent with the Porton Downs tests in that no large particles were detected in these studies. There are three possible explanations for the difference. The first is a possible bias toward the smaller drops produced by the experimental technique used. For example, the holographic station recorded droplets in the center of the test cell; if larger droplets were located outside of the core flow, due either to gravitational settling or unusual flow patterns, they would be lost to the holographic exposure.

The second possibility is that the droplet sizes recorded at this distance downstream are representative of the state of the fuel, and a process of coalescence occurring further downstream would account for the appearance of larger droplets. Wigg (Ref. 7) supports this argument from his work with large air-blast atomizers in which he notes a variation in droplet size as a function of the location of the sampling station. Merrington, et al. (Ref. 8) also noted that they observed larger droplets as they moved downstream. These observations prompted the short experimental program to investigate the possibility of coalescence which is reported in Section 4.0.

The third consideration is addressed to the problem of comparing the variations in the parameters under which the various tests were conducted. The defoliant studies injected similar mass flow rates of liquid into the airstream; however, the airstream velocity was almost twice that of the actual fuel dump test. Wasson, et al., were able to match the air speed but were forced to reduce the mass flow rate of the liquid due to limitations of the wind tunnel pumping system.

In order to evaluate the significance of these differences, it is necessary to postulate the nature of the atomization process. Numerous theories have been presented concerning the mechanism by which a liquid jet breaks up and forms droplets. The classical work of Rayleigh (Ref. 9) considers the buildup of ripples on the liquid surface and associates an eventual droplet size to the wavelength of this disturbance.

However, this approach is not deemed applicable in considering large diameter liquid jets encountering high-speed airflows. Photographs of liquid jets encountering airstreams of various velocities are presented by Nukiyama, et al. (Ref. 10). The photographs show high-speed airstreams stripping fine ligaments from the liquid surface and a subsequent breakup of these ligaments into droplets. While the liquid jet diameters studied by Nukiyama are smaller than those under consideration for fuel dumping, this breakup mechanism is considered the most likely process of atomization.

Accepting this method of atomization then one can postulate a sequence of events as the liquid jet enters the airstream. The initial stripping of ligaments from the outer surface not only produces an initial quantity of droplets but in turn accelerates the bulk of the liquid core such that the secondary ligaments are produced with a slightly reduced relative airspeed. One can consider this process being repeated until either the liquid core is depleted or the velocity difference between the liquid and the airstream is reduced sufficiently so that further breakup would occur as a result of instabilities in the liquid core as suggested by Rayleigh. While the orderly shedding of successive layers of liquid is obviously compromised by the extreme turbulence caused by the injection of the liquid into the airstream, the model would indicate that the droplets produced from the initial exposure of the liquid to the airstream should be independent of the jet diameter. It would also indicate that minimum droplet sizes would be primarily defined by the relative velocity between the initial liquid jet and the airstream and the physical properties of the liquid. Castleman

(Ref. 11) suggests that for gas-liquid velocities above 100 m/sec this minimum size is only a function of the liquid properties and gives a value of 10 μm for water droplets. Sauter (Ref. 12) reports a minimum value of 7 μm for kerosene droplets.

Since the three tests under consideration were conducted with relative velocities between the liquid and airstream in excess of 100 m/sec, then one would expect the droplet-size distribution to start with droplets around 5- to 10- μm diameter.

Predictions for an expected mass median or maximum droplet size for the various tests are open to serious question since no theoretical treatment is available to handle the problem, and semi-empirical relations have all been developed with data obtained from studies investigating much smaller fluid jets.

Many investigators have given a dimensional analysis of the break-up of liquids into droplets (Ref. 13). Using this approach one can assume that the average droplet size can be expressed as

$$KD, \rho_l, V, \sigma, \mu_l, \rho_g, \mu_g$$

Expressing these variables in the form of a power series, they may be rearranged to yield the following equation with four nondimensional groupings,

$$d = Da \left(\frac{\sigma}{V^2 \rho_g D} \right)^a \left(\frac{\mu_l}{\rho_l D V} \right)^b \left(\frac{\rho_g}{\rho_l} \right)^c \left(\frac{\mu_g}{\mu_l} \right)^d$$

where α , a , b , c , and d are appropriate constants. Using this approach, Ingebo, et al. (Ref. 14) present the expressions,

$$d_{av} = 3.9D \left(\frac{We'}{Re'} \right)^{0.25}$$

and

$$d_{max} = 22.3D \left(\frac{We'}{Re'} \right)^{0.29}$$

where

$$We' = \frac{\sigma}{v^2 \rho_g D} \quad (\text{Inverse Weber number})$$

and

$$Re' = \frac{D v \rho_l}{\mu_l} \quad (\text{Liquid film Reynolds number})$$

The experiments from which these constants were determined covered the range of airstream velocities of interest in the atmospheric dumping problem as well as matching the properties of the fuel. However, the diameter of the initial fluid jet was almost two orders of magnitude smaller. While one might hesitate to apply this work directly to the large-scale dumping, it is of interest to note how these equations would predict the trend of the droplet sizes as a function of the initial liquid jet diameter. Curves from these equations are presented in Fig. 2. For the conditions of the full-scale atmospheric fuel dumps (Ref. 4), these equations predict a median droplet size of $360 \mu\text{m}$ and a maximum size of $670 \mu\text{m}$. These values compare to 240 and $400 \mu\text{m}$ as reported.

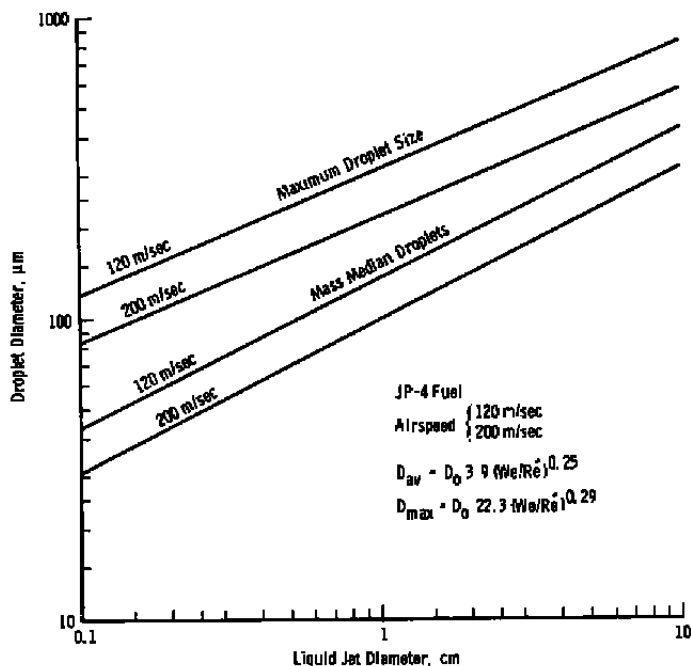


Figure 2. Droplet size as a function of liquid jet diameter.

The upper limit of the droplet size (which might survive a fuel dump and free fall) can be estimated by referring to the work by Volynski (Ref. 15) and similar studies by Lane (Ref. 16). These studies define a critical Weber number at which a single droplet will become unstable and break up. Using Volynski's critical value of $W_e = 7$, then one can plot the maximum stable drop size as a function of ΔV or the relative velocity between the JP-4 and the airstream. Such a curve is presented as Fig. 3. Assuming that such a large droplet can survive the dumping process, then one can estimate the resulting terminal velocity of the droplets in free fall (Ref. 17). Figure 4 presents a plot of terminal velocities along with the critical velocities as predicted by Volynski and Lane. This indicates a maximum droplet size between 3250 and 3750 μm and is based on the terminal velocity of spherical droplets. It is obvious that serious distortion must occur in liquid droplets prior to breakup, and thus, some modification of the terminal velocity curve should be made.

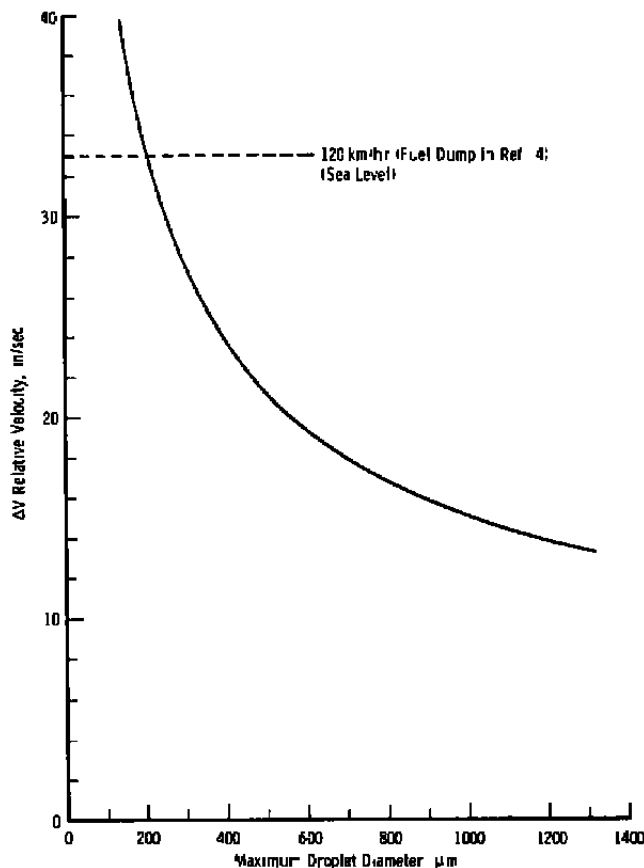


Figure 3. Maximum droplet size as a function of relative velocity.

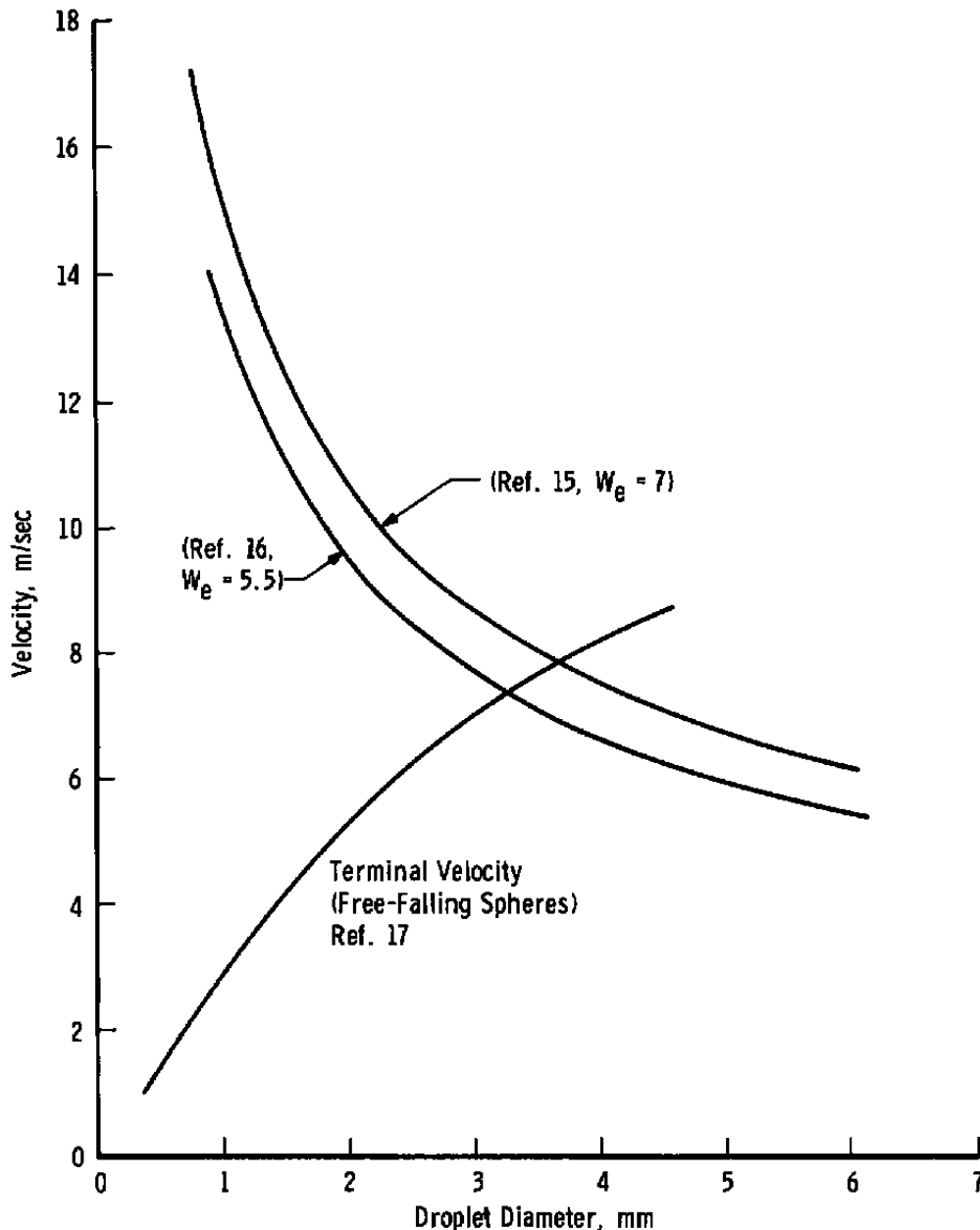


Figure 4. Critical velocity for droplet breakup.

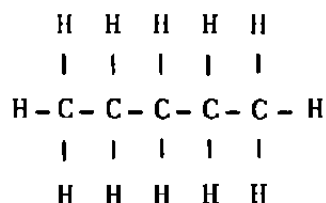
For lack of more definitive data at the present time it is suggested that the most likely droplet size distribution would consist of that obtained by Cross, et al. (Ref. 4) modified by including an additional 35 percent of the fuel in the form of droplets in the size range from 10 to 50 μm . A suggested size distribution is presented in Fig. 1 which reflects this modification.

One further parameter of concern in considering the aerodynamic properties of the jettisoned JP-4 is the drag coefficient of the free-falling droplets. Gunn and Kinser (Ref. 18) and Laws (Ref. 19) present data for falling water droplets which show a considerable difference in drag coefficient from that of solid spheres. How much of the difference can be associated with evaporation of the liquid and how much can be considered to be caused by aerodynamic deformation of the droplet is not known. Data from which the drag coefficient of liquid droplets may be computed is extremely limited, and no information could be found which might apply to droplets of JP-4 under free-fall conditions. Thus, a series of experiments to determine the drag coefficient of JP-4 in free fall at various simulated altitudes was conducted and is reported in Section 5.0.

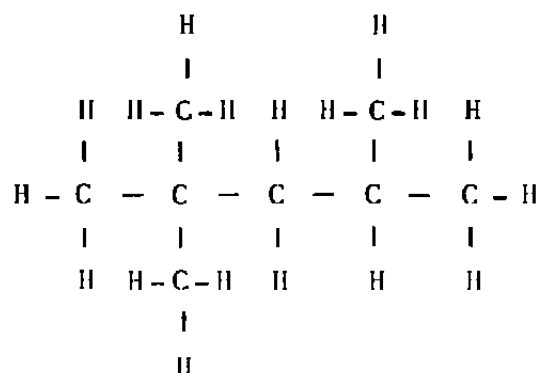
3.0 PROPERTIES OF JP-4 FUEL

The present specifications for JP-4 fuel have been developed over a number of years. They represent an acceptable compromise between many of the conflicting requirements for the ideal fuel. For example, a high volatility is desirable for engine starting and cold weather performance. However, a low volatility is preferred by the fuel system designer who has to consider vapor locking in pumps and the problems of foaming and excessive venting from fuel tanks during high rates of climb. One important factor which must be considered is that a usable fuel must be available worldwide for effective military operations and a too narrow set of specifications significantly reduces the availability. Because of these factors, JP-4 fuel is not defined in terms of specific components but by some general characteristics. It is a kerosene-type fuel with a wide boiling range. It may contain as many as 5,000 to 10,000 hydrocarbons. These can be divided into three general categories: paraffins, aromatics, and olefins.

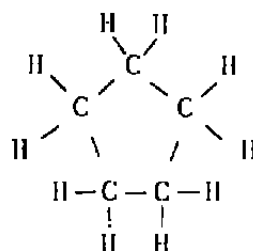
The paraffins constitute 75 to 90 percent of JP-4 fuel. They are stable in storage, clean burning, and do not attack the common elastomers used for gaskets and O-rings. Typical paraffins are straight chain paraffins such as n-pentane, branched chain paraffins such as 2, 2, 4 trimethyl pentane, and cycloparaffins such as cyclopentane.



(n-pentane)

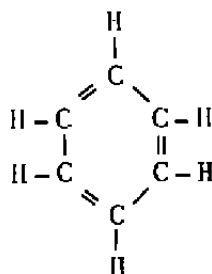


(2-2-4 trimethyl pentane)

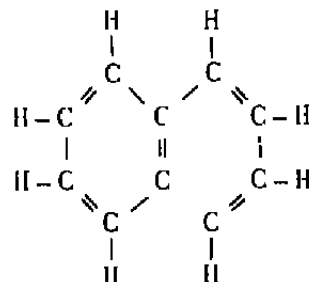


(cyclopentane)

The aromatics are characterized by the six-member benzene ring. They are stable in storage, smoky burning, and have high solvency powers. The concentrations of aromatics are limited to 25-percent maximum, though most fuels contain only 10 to 15 percent. Benzene and naphthalene are typical of the aromatics.

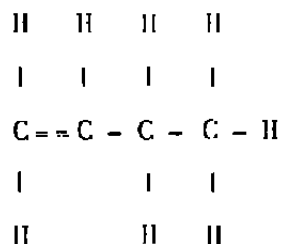


(benzene)

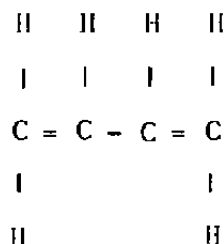
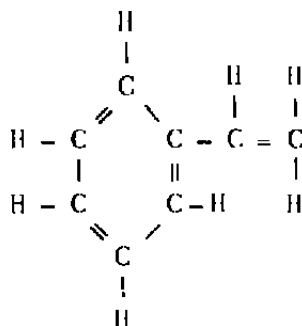


(naphthalene)

The olefins are hydrocarbons with a characteristic carbon-to-carbon double bond. This double bond is more reactive chemically than the double bonds in the aromatic hydrocarbons. The olefins are limited to a maximum of 5 percent in JP-4 fuel. Some types of aromatic olefins and diolefins are very reactive in the presence of atmospheric oxidants, usually these constitute less than 0.2 percent of JP-4. Typical olefins are butane, butadiene, and styrene.



(butane)

(butadiene)
(diolefin)

Styrene (aromatic olefin)

The physical properties of JP-4 are generally defined by MIL-F-5624H (Table 2).

3.1 DENSITY

The fuel density is of prime interest in aircraft design in the determination of location of fuel tanks and calculating flight range. In the particular case of fuel dumping, the density is required in calculating the fallout rates of the resultant droplets. The allowable specific gravity

range is from 0.751 to 0.802 although the average of fuels (>5000 samples) measured in 1970 indicates a value close to 0.76 (Ref. 20). Using this average value, Fig. 5 presents a plot of specific gravity as a function of temperature over the range of interest for JP-4 fuel free falling in the atmosphere. In those instances where the density is reported in °API, the values can be converted to specific gravity by using the relation

$$\text{Specific gravity } (60^{\circ}/60^{\circ}\text{F}) \approx \frac{141.5}{(15^{\circ}/15^{\circ}\text{C}) \text{ } ^{\circ}\text{API} + 131.5}$$

Table 2. Specifications of JP-4

Requirements	JP-4 (NATO F-40)
Distillation	
Fuel evaporated 20 percent minimum at	290°F (143.3°C)
Fuel evaporated 50 percent minimum at	370°F (187.8°C)
Fuel evaporated 90 percent minimum at	470°F (243.3°C)
Maximum residue, Vol. percent	1.5
Distillation loss, Vol. percent maximum	1.5
Gravity °API, minimum (sp gr max)	45.0 (0.802)
Gravity °API, maximum (sp gr min)	57.0 (0.751)
Existent gum, mg/100 ml maximum	7
Sulphur, total percent weight maximum	0.4
Vapor pressure, 100°F psi minimum	2.0
Vapor pressure, 100°F psi maximum	3.0
Freezing point, maximum	-72°F (-58°C)
Heating value, Btu/lb minimum	18,400
Aromatics, Vol. percent maximum	25.0
Olefin, Vol. percent maximum	5.0
Particulate matter, mg/gal maximum	4.0
Icing inhibitor, Vol. percent maximum	0.15
Icing inhibitor, Vol. percent minimum	0.10
Total acid number, maximum	0.015

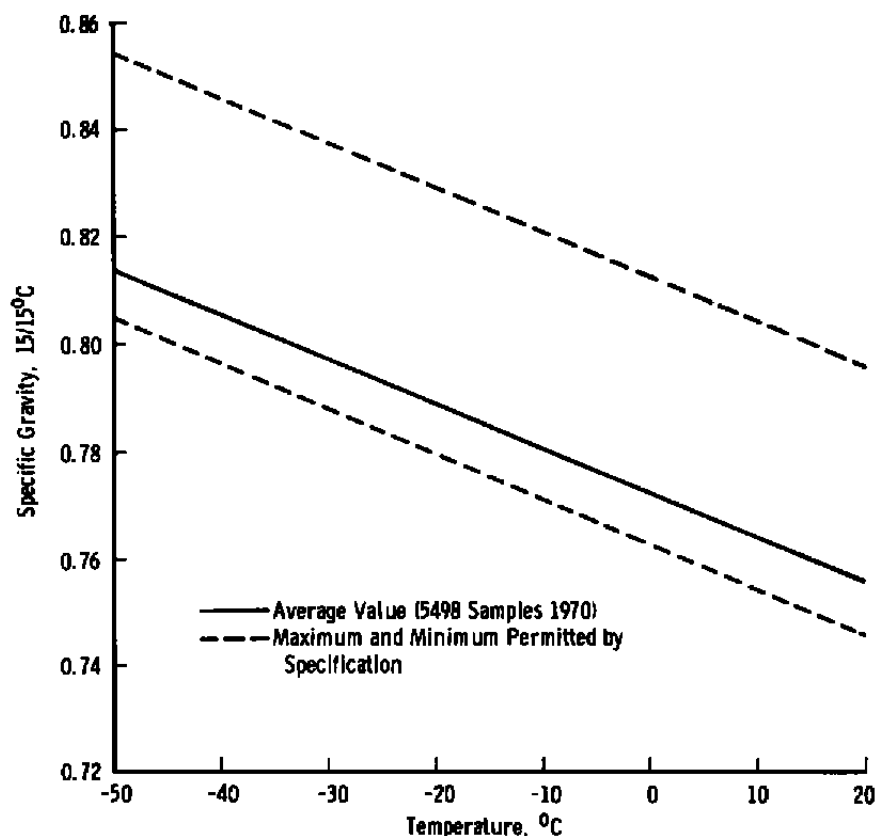


Figure 5. Specific gravity of JP-4 versus temperature.

3.2 VAPOR PRESSURE

The volatility of JP-4 fuel is controlled by specifying the ASTM distillation curve (D86-52) and the Reid vapor pressure. The distillation curve is used to indicate the overall volatility of the fuel, and the Reid vapor pressure indicates the initial tendency of the fuel to vaporize. Neither test gives absolute values of vapor pressure.

The distillation tests are run with 100 cc of fuel in a closely prescribed apparatus and at a controlled distillation rate. Vapor temperatures are recorded at the head of the condensing tube as various percentages of the fuel are distilled and collected in a receiver. This process does not give the temperature for initial boiling, does not isolate any of the fuel components, nor give any information as to the final boiling point. It is, however, a reproducible process and has been accepted as a general means of comparing various fuel blends.

The Reid vapor pressure is determined by sealing one volume of fuel and four volumes of air in a closed vessel and raising the temperature to 37.78°C (100°F). The resulting pressure reported in psia is noted as the Reid vapor pressure. For JP-4 the specifications set the limits between 2 and 3 psia. Data obtained for the period from 1964 to 1970 show average values of 2.6 psia (>5000 samples each year) (Ref. 20).

The classical vapor pressure-temperature relation is expressed by

$$\log P = A - B/T$$

where

P = absolute pressure

A,B = constants

T = absolute temperature

For the hydrocarbons of interest, the constant B can be associated with the normal boiling point of the pure compound. Figure 6 is a plot of vapor pressure versus temperature for several typical hydrocarbons. The abscissas are scaled as the negative of the reciprocal temperature in order to present a set of linear curves. A comprehensive plot of curves for hydrocarbons with normal boiling points from 100 to 1200°F is presented in Ref. 21. The vapor pressure for ideal mixtures of hydrocarbons can be calculated using Raoult's Law. However, the wide range between the boiling points of the most volatile and least volatile components in JP-4 plus the overwhelming number of specific compounds present a problem in using this approach. Empirical equations to calculate the vapor pressure of JP-4 as a function of temperature have been developed which use various combinations of the ASTM distillation data, the normal boiling point temperature, the Reid vapor pressure, and the flash point temperature. These equations are presented in Ref. 22, and a plot of the vapor pressure of an average JP-4 using this approach is included in Fig. 6. These empirical equations describe only 100-percent JP-4 and are not applicable for residues of JP-4 which would be encountered, for example, in an evaporating droplet.

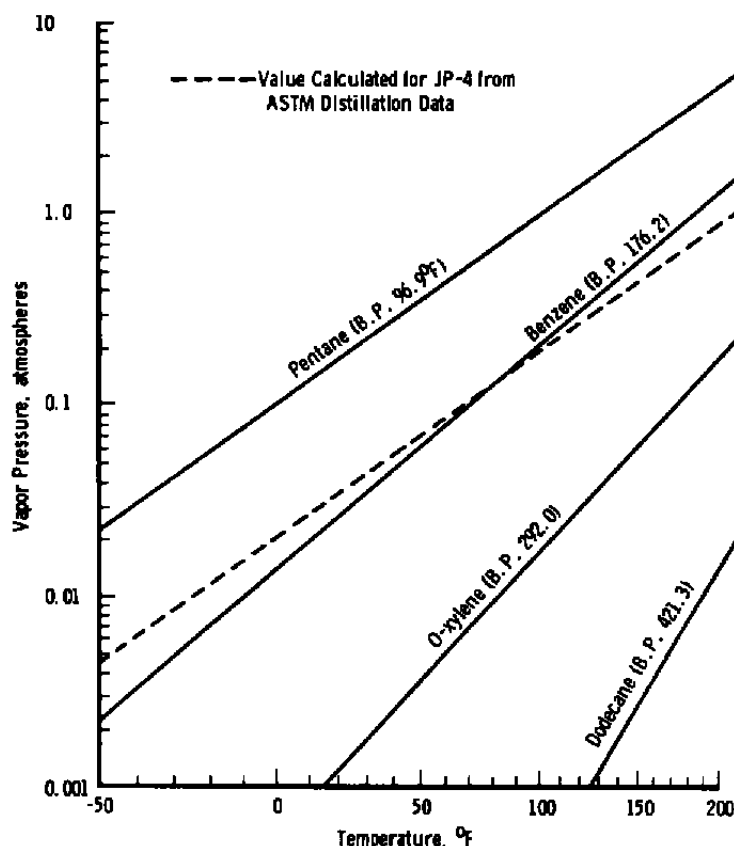


Figure 6. Vapor pressure of various hydrocarbons.

3.3 SURFACE TENSION

The surface tension for many of the hydrocarbons can be determined from their molecular weight, critical temperature, and density. The equation developed by Ramsey and Shields (Ref. 23) is given as

$$\sigma = \left(\frac{\rho}{M}\right)^{2/3} 2.12 (T_{cr} - 6 - T)$$

where

σ = surface tension (dynes/cm)

ρ = density (gm/cc at temperature T)

T = temperature of liquid (°K)

T_{cr} = critical temperature (°K)

M = molecular weight

The values of surface tension for JP-4 reported in Ref. 22 are based on this approach.

The molecular weight and the critical temperature for JP-4 are determined from the general correlations between density, average molecular weight for normal paraffins, molecular weight and critical temperature as given in Ref. 21.

The values of surface tension calculated for the paraffins agree with the curves presented in Ref. 22. However, the values calculated for the aromatics show considerable variance. Figure 7 presents values for octane and o-xylene as a typical paraffin and aromatic. While the aromatics in JP-4 are limited to 25 percent by volume and in actual samples average at approximately 11 percent, this may be sufficient to significantly affect the actual value of the surface tension. In those areas where the surface tension is a significant parameter, caution should be used in accepting the calculated values based on the specific gravity of the JP-4.

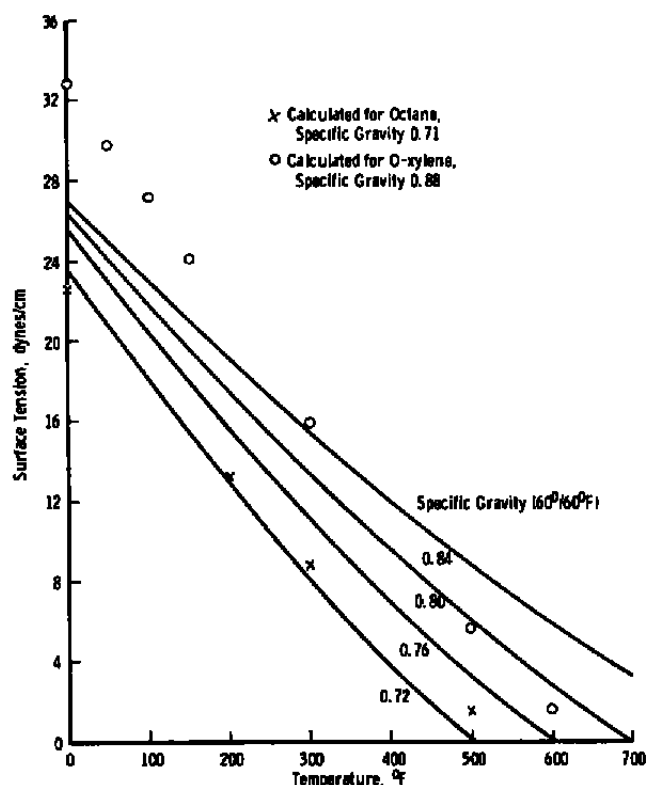


Figure 7. Surface tension as a function of temperature.

3.4 LATENT HEAT OF VAPORIZATION

The latent heat of vaporization is the difference in enthalpy between the liquid and the vapor phase at constant temperature. Maxwell (Ref. 21) presents a method for determining the latent heat of vaporization of a mixture of hydrocarbons by using the volume average boiling point of the mixture and the average molecular weight and using these values to modify the latent heat of vaporization curve of a comparable normal paraffin. Using this technique, a plot of latent heat of vaporization as a function of temperature for an average JP-4 is presented in Fig. 8. In essence, this is a slightly modified curve of the heat of vaporization of iso-octane. This assumes the complete vaporization of JP-4 and thus is not directly applicable for the fractional evaporation of JP-4 as is considered in the free fall of JP-4 droplets. However, this same technique can be applied to each fraction of the JP-4 and a series of such curves can be generated. At the temperatures considered for the free-fall evaporation of JP-4, the enthalpies of the individual components of a mixture are additive in the liquid phase and in the vapor phase. Thus, the latent heat of vaporization of JP-4 fractions can be modeled by using a mixture of hydrocarbons, each one of which is representative of a specific fraction.

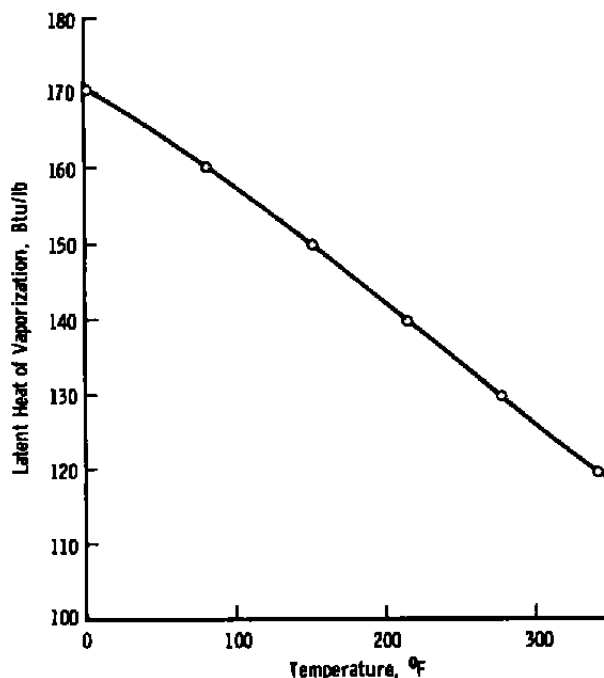


Figure 8. Latent heat of vaporization of JP-4.

3.5 SPECIFIC HEAT

The specific heat of hydrocarbon liquids can be correlated to their specific gravity with a small correction for the volume average boiling point (Ref. 21). For convenient reference, the curves applicable to JP-4 are presented in Fig. 9.

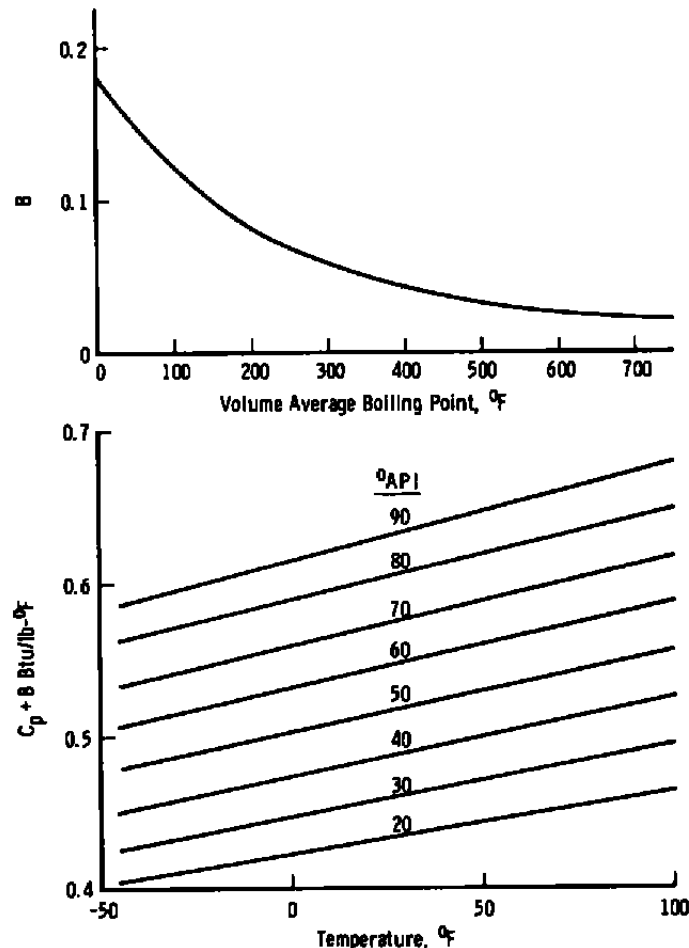


Figure 9. Specific heat as a function of temperature.

4.0 DROPLET BREAKUP AND COALESCENCE

A short experimental program was conducted to look at the breakup of a liquid stream and to determine if coalescence of droplets was a significant factor in the fuel-dumping process.

The apparatus consisted of a concentric air nozzle and liquid feed tube. The liquid was supplied from a pressurized reservoir. Various liquid flow rates and liquid exit velocities could be obtained by adjusting the reservoir pressure or by changing the exit diameter of the flow tube. The air was supplied from a bank of high-pressure tanks and its flow velocity at the exit of the nozzle was adjusted by a valve in the supply line. Air velocities were calculated from pitot tube measurements made at the exit plane of the nozzle with no liquid flow.

The air-liquid nozzle assembly was mounted about four feet from the ground and pointed upward at a 45-deg angle. A strip of paper, 18 in. wide and 50 ft long, was placed on the floor along the centerline of the nozzle assembly. The reservoir was filled with liquid (water or JP-4) to which had been added a little dye. Flow rates of the liquid were measured by pressurizing the reservoir and then opening the supply valving and timing the liquid as it discharged into a calibrated container. No airflow was used during this calibration.

The data were taken by adjusting the airflow through the nozzle to obtain the desired velocity and then starting the liquid flow. The liquid flow was continued for approximately five seconds and then terminated. The airflow was then shut off and the paper strip set at one side to dry. The droplets which settled on the paper left a colored imprint from the dye and provided a permanent record of the droplets.

The approximate size of the droplets which left the circular stains was determined by dropping known volumes of the dyed liquid onto the paper. This was accomplished by drawing a small quantity of liquid into a finely drawn glass capillary. The diameter of the capillary and the length of liquid was measured with an optical comparator. This known volume of liquid was then expelled as a droplet whose diameter was calculated from the known volume of liquid released from the capillary. In addition to this method of sizing, small dishes of silicon oil were spaced along the paper during the tests with water, and samples of the droplets were viewed and measured directly with an optical comparator. While not extremely accurate, it is felt that droplets as small as $40\ \mu$ in diameter could be detected. No liquid was found which could be used with the JP-4 to retain the individual droplets.

The droplet sampling technique used for these tests does not permit a determination of a droplet size distribution. However, it does give some indication of maximum droplet sizes and more important it confirms trends in the size distribution as influenced by varying selected parameters. The range of flow variables investigated is indicated in Table 3.

Table 3. Droplet Data Produced from Spray Tests

Run No.	Air Velocity, m/sec	Liquid Velocity, m/sec	Liquid Flow Rate, kgm/min	Max Droplet size, μ
1	140	4.3	4.5	2600
2	140	1.7	1.8	1750
3	140	8.6	12.7	2550
4	75	8.0	0.4	1100
5	75	8.6	12.7	2600
6	140	1.1	1.2	600
7	140	4.3	4.5	2500
8	75	13.7	0.7	1250
9	75	4.3	4.5	2550
10	75	1.7	1.8	2600
11	140	4.3	4.5	2650
12	140	19.9	1.2	650

4.1 BREAKUP OF LIQUID JET

The following general observations are noted:

- For comparable flow conditions, the droplets of JP-4 were consistently smaller than the water droplets. The ratio of the largest JP-4 to water droplet, for comparable runs, ranged from 0.69 to 0.76. This compares favorably with a value of 0.63 predicted by Ingebo's empirical equation.
- There were no other significant differences in the behavior of JP-4 and water as flow parameters were varied.
- Over the range of parameters varied, there was no observable change in the smaller droplet sizes. For the higher liquid flow rates and the lower air velocities the density (number of droplets per cm^2) increased, but the size range at the station nearest the nozzle exit remained at 40 to 100 μm .
- Runs with similar air velocity and liquid velocity but different mass flow rates of liquid (e.g., No. 4 and

No. 5) indicated a wider spectrum of droplet sizes at midfield, and a larger maximum droplet size in the far field for the higher flow rate.

- e. Comparing runs No. 2 and No. 10 indicated that the difference in airspeed had a significant effect on the maximum size of the droplets produced. However, a similar comparison between runs No. 3 and No. 5 show no such effect on the maximum droplet size. The only difference between the data in runs No. 3 and No. 5 is that the larger droplets were recorded 25 percent farther downstream in run No. 3. These data indicate that the maximum droplet size is a function of the relative airspeed up to the point where the mass loading of the liquid is so large that the energy available in the zone of interaction between the high-speed airstream and the liquid is insufficient to atomize all of the jet. This results in relatively large fragments of liquid traveling at modest velocities and subsequently breaking up due to internal instabilities as they free fall. This secondary process of breakup would also account for the consistent upper limit of droplet size observed during these tests.
- f. Comparison of runs No. 6 and No. 10 indicate no significant difference in droplet size due to the change in the liquid velocity. This might be expected since the relative velocity between the airstream and the liquid does not change appreciably.

The most notable feature in the data was the fact that droplets from 40 to 100 μm were recorded nearest the nozzle and the farther the distance downstream the larger the droplet size became. For most conditions, no 40- to 100- μm droplets were noted beyond 15 ft, and droplets $> 2000 \mu\text{m}$ were all recorded at distances beyond 25 ft. It is suspected that previous investigators have seen this same effect and suggested that coalescence of small drops is responsible for the larger drops appearing downstream (Refs. 7 and 8). Visual observation of the droplet cloud, however, indicates that this droplet sizing is primarily due to the fact that once the initial droplets are sufficiently far removed from the exhausting airstream, the quiescent atmosphere acts as a selective filter. The smaller drops are rapidly decelerated and thus fall out nearer to the nozzle while the larger drops travel much further downstream.

4.2 COALESCENCE OF DROPLETS

The apparatus was modified slightly to study the possibility of coalescence of droplets. The air supply was saturated with oil vapor prior to exhausting through the nozzle, and small petrie dishes filled with 40W oil were used to collect the sample droplets. Only water droplets were studied although it is suggested that the observation would apply equally as well to JP-4.

Using the same experimental procedures of establishing airflow then starting the liquid flow for a 5-sec period, samples of droplets were collected and immediately examined under a microscope.

It was observed that many of the larger droplets $>750\text{ }\mu\text{m}$ had numerous (5 to 25) small 40- to $50\text{-}\mu\text{m}$ droplets adhering to their surface. It was also noted that under all the conditions tested and in the many sample dishes examined, that there were no aggregations of small droplets without the large parent droplet.

Single droplets of water were produced by a hypodermic needle and dropped from heights up to 40 ft into similar oil-filled collectors. These droplets were also examined and no evidence of breakup or formation of these small satellite droplets was found.

It is suggested that this experiment shows that larger drops moving through a field of small droplets collect some of the smaller droplets. Normally, these droplets would lose their identity as they merged with the larger drop; however, in these tests the surface contamination caused by the oil vapor in the air supply prevented this assimilation. Since no clusters of small droplets alone were found, these observations indicate that large drops are not produced by coalescence of small droplets. However, it is also apparent that larger drops do grow by collision with and assimilation of smaller droplets.

5.0 DRAG COEFFICIENT OF FREE-FALLING DROPLETS

The experiments conducted by Gunn, et al. (Ref. 18) and Laws (Ref. 19) show that the drag coefficient for water droplets differs significantly from the "standard" curve for solid spheres as published by Schlichting (Ref. 17) and Hoerner (Ref. 24). However, there is considerable variation in the value of the drag coefficient for solid spheres as reported by individual investigators. Bailey (Ref. 25) presents a

review of the various data in the literature and suggests that much of the variation can be associated with the type of support or sting used in many of the experiments. From this survey, and subsequent work he conducted in a ballistic range, Bailey proposes a modified "standard" curve.

5.1 EXPERIMENTAL APPARATUS

In order to provide drag coefficient data for free-falling JP-4 droplets the following apparatus was constructed. A vertical tube approximately 36.5 m in length by 8 cm in diameter was installed in the stairwell of the Mark I test building. Viewports with instrumentation feedthroughs were installed at approximately 3-m intervals along the length of the tube. A small chamber, housing the droplet-producing and detection system, was located at the top of the drop tube and is shown schematically in Fig. 10. The complete system was vacuum tight, and internal pressures could be preset to simulate altitudes from sea level to 30,000 m.

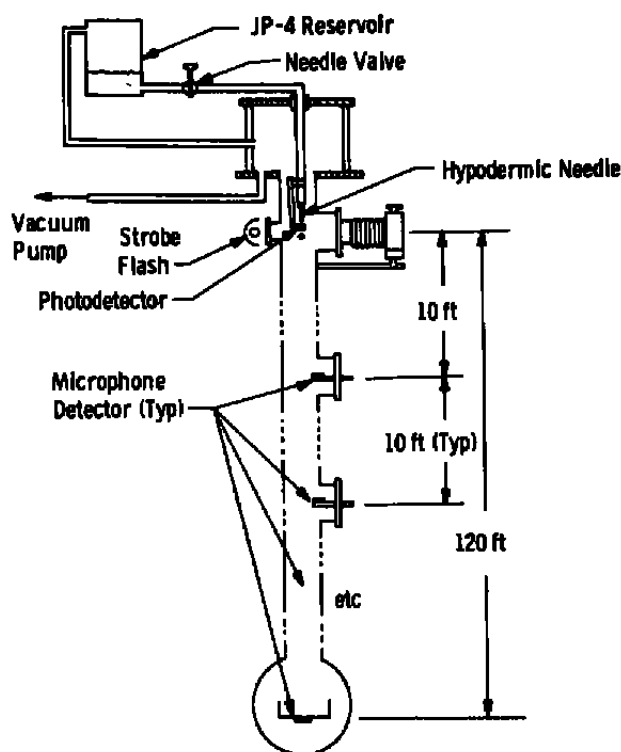


Figure 10. Schematic of drop tube.

Several methods for producing droplets were evaluated. A vibrating needle system produced adequate droplets; however, there was sufficient horizontal momentum added to the droplets that they would not fall the full 36 meters without hitting the side of the tube. The system finally selected was a simple gravity-fed set of hypodermic needles which had been modified by cutting off their tapered tip and carefully buffing and polishing the squared end. It was noted that any asymmetry about the end of the needle apparently caused the droplet to rotate as it fell with the result that the droplet would swerve and impact with the wall. The rate at which the droplets were produced was controlled by a micrometer screw which adjusted the height of the JP-4 reservoir. The top of the reservoir was vented into the chamber on the drop tube so that adjustments of the pressure in the system to simulate various altitudes would not affect the droplet formation rate. For most of the data taken, the droplet formation rate was one per eight seconds.

The droplets were timed during their free fall with a crystal controlled digital counter. A starting trigger was produced as the droplet was released from the needle and fell between an LED and a companion photodetector. This pulse coupled through a suitable delay also activated a strobe light which was used to backlight and photograph the droplet as it passed a viewport. A reference wire of known diameter was included in the field of view of the camera and in the same focal plane as the droplet. The droplet diameters were obtained from these films using a microscope and an optical comparator. A cross check on this method of sizing droplets was made by collecting and weighing a series of droplets and then comparing the calculated average drop size with that determined from photographs. Droplet diameters calculated by the weighing method were 1 to 2 percent smaller than those determined from photographs. This could be due to slight losses caused by evaporation of JP-4 during the collecting and weighing operation. The slight differences were not considered to warrant further investigations, and the photographic method to determine diameter was used in all subsequent tests.

Each station down the drop tube was fitted with a thin metal butterfly valve to which was cemented a small crystal microphone. The time of flight to a particular station was recorded by closing the valve at that station and using the impact of the droplet on the valve as recorded by the microphone. The time of flight of several hundred droplets to each station was taken for each altitude simulation and each droplet size. The data were treated statistically to obtain the average value for the terminal velocity of a particular size drop falling in the tube under specific atmospheric pressures.

5.2 RESULTS

The first runs were conducted with water droplets so that the data generated using this apparatus could be directly compared with those of Gunn, et al. A typical velocity profile is presented in Fig. 11. These data are included on the plots of drag coefficient versus Reynolds number in Figs. 12 and 13. The experiments were repeated using JP-4 and the results are presented in Figs. 12 and 13.

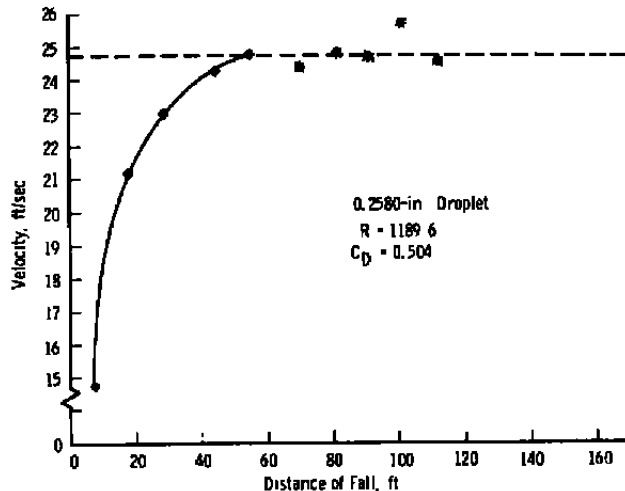


Figure 11. Velocity profile of falling water droplet.

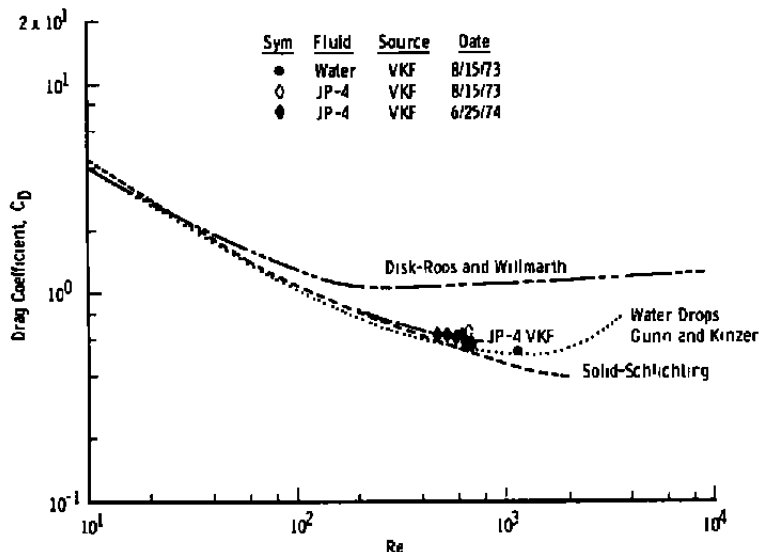


Figure 12. Plots of drag coefficient versus Reynolds number for disks, spheres, (solid and liquid) and water droplets.

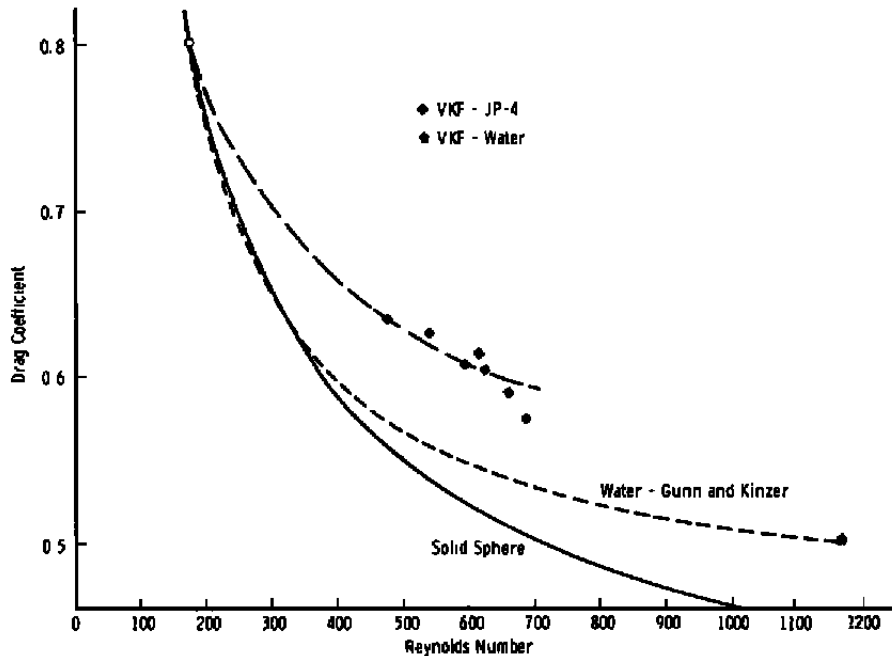


Figure 13. Drag coefficient versus Reynolds number for JP-4 droplets.

5.3 DISCUSSION

Two factors can be considered as possibly modifying the drag coefficient of falling JP-4 droplets. The first is the evaporation of the more volatile components which are added to the boundary layer and wake. However, a limited number of experimental runs with a fraction of JP-4, from which the most volatile 10 percent of the hydrocarbons had been removed, showed no measurable change in terminal velocity. It is therefore suggested that this effect is of minor importance. The second is the deformation of the droplet due to aerodynamic forces. This is emphasized by both Spilhaus (Ref. 26) and Magono (Ref. 27) in their studies of free-falling water droplets.

The resultant droplet shape is determined by the interaction of the surface tension force (σ_ℓ/r_ℓ) which tends to maintain the spherical shape and the pressure forces $\rho_g V^2$ tending to deform it. The ratio of these forces has been designated as the Weber number, $W_e = \rho_g r_\ell V^2 / \sigma_\ell$. Hinze (Ref. 28) presents a mathematical analysis of the deformation of

liquid droplets and, assuming that the distortion produces an ellipsoidal shape, predicts a maximum flattening given by

$$\left(\frac{\delta}{r_0}\right)_{\max} = -0.095 \text{ Re}$$

where δ is the difference between the length of the minor axis of the ellipsoid and the radius of the undistorted spherical droplet (r_0).

5.4 APPLICATION OF DATA TO ATMOSPHERIC TESTS

Given the atmospheric conditions, the terminal velocity for a given droplet size can be computed using the following technique. Since at terminal velocity the aerodynamic drag forces and the gravitational forces are equal, then

$$C_D \frac{1}{2} \rho_g V_t^2 \pi r^2 = \frac{4}{3} \pi r^3 \rho_l g$$

or

$$C_D = \frac{8}{3} \frac{\rho_l \mu_l g}{\rho_g V_t^2}$$

By definition

$$\text{Re} = \frac{2 r \rho_g V_t}{\mu_g} \quad (1)$$

Combining these terms to eliminate V_t yields

$$\text{Re} \sqrt{C_D} = \sqrt{\frac{4}{3} \frac{\rho_l \rho_g \mu_l^3}{\mu_g^2}} \quad (2)$$

Figure 14 is a plot of Re versus $\text{Re} \sqrt{C_D}$ made from the data obtained for JP-4 in these tests. As can be seen, the data can be represented by the linear equation

$$\text{Re} \sqrt{C_D} = 0.73 \text{ Re} + 28.6 \quad (3)$$

Therefore, inserting the atmospheric parameters and the droplet diameter in Eq. (2) yields a value for $Re\sqrt{C_D}$. This value can be used in Eq. (3) to determine the appropriate Reynolds number to use in Eq. (1). Equation (1) can then be solved to give the terminal velocity.

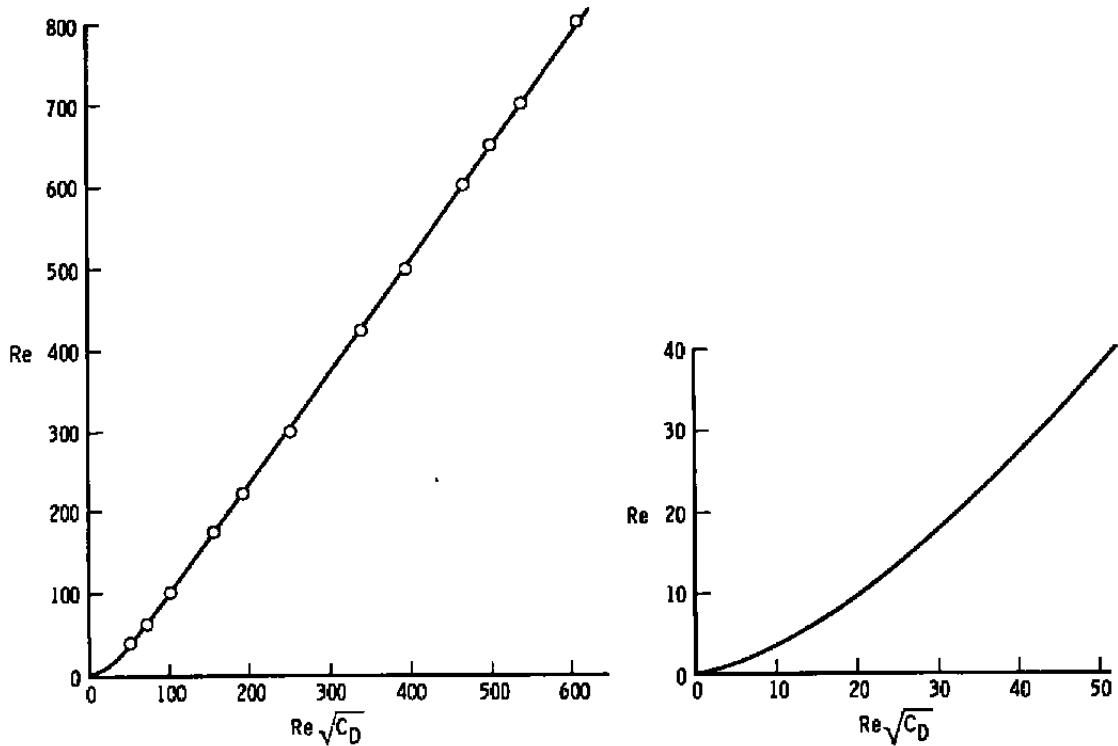


Figure 14. Plot of Re versus $Re\sqrt{C_D}$ for JP-4.

Using a similar approach, the drag coefficient C_D and the Reynolds number Re can be combined to yield

$$\frac{C_D}{Re} = \frac{4.3 \mu_g \rho_l g}{\rho_g^2 v_l^3} \quad (4)$$

Figure 15 is presented as a plot of Re versus C_D/Re as determined from the drop tube tests for JP-4 fuel droplets. Thus, inserting observed values for the parameters in Eq. (4) yields a value of C_D/Re which can be associated with an appropriate Reynolds number from Fig. 15. This Reynolds number can then be used to calculate the appropriate droplet size.

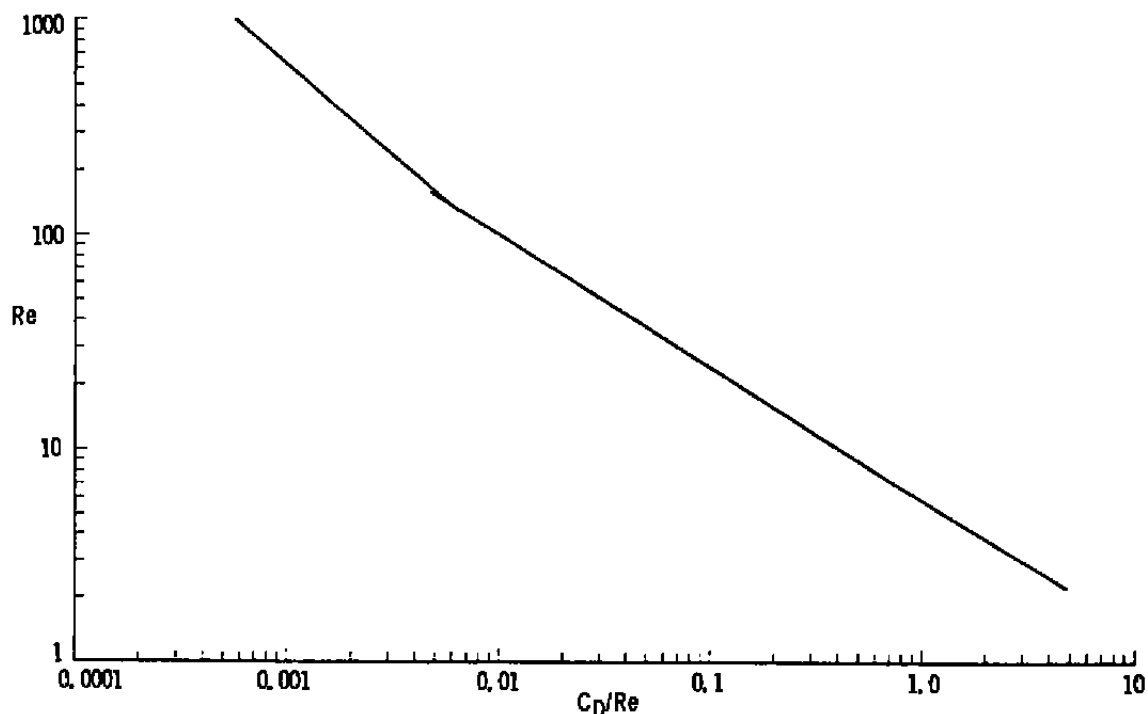


Figure 15. Plot of Re versus C_D/Re for JP-4.

6.0 EVAPORATION OF JP-4 DROPLETS

After the initial breakup and aerodynamic dispersion of the JP-4 droplets in the aircraft wake, the initial distribution of the hydrocarbon vapors throughout the atmosphere will be controlled by the evaporation characteristics of the free-falling droplets. Attempts to solve the equations for the evaporation of a volatile liquid sphere in a moving gas stream have met with limited success. Frössling (Ref. 29) presented the first semi-empirical results indicating that

$$\frac{dm}{dt} = -2\pi D^* \frac{MP}{RT} d[1 + K(S_c)(Re)^{1/2}]$$

where

D^* = diffusion coefficient

M = molecular weight of liquid

P = vapor pressure at temperature T

T = liquid temperature

d = droplet diameter

S_c = Schmidt number = $\rho \frac{D^*}{\mu}$

and

$$K(S_c) = 0.276 S_c^{1/3}$$

Further, workers such as Rang (Ref. 30) have modified this approach to include heat-transfer effects. However, the difficulties added by the complex multicomponent nature of JP-4 fuel would seem to be well beyond the scope of such analytical treatment.

In an attempt to reduce the problem to tractable form, Lowell (Refs. 31, 32, 33, and 34) made the assumption that JP-4 could be modeled by a mixture of 10 selected hydrocarbons and that the evaporation rate of such a droplet could be calculated by summing the evaporation of the specific components. The general scheme used was to consider the droplet diameter and temperature fixed for a short interval of time. During this time step, the terminal velocity and Reynolds number of the falling droplet was calculated. The Nusselt number of mass transfer was then calculated and the mass-transfer coefficient for each constituent was then obtained from the Nusselt number. The vapor pressure of each component was then used along with the appropriate mass-transfer coefficient to determine the mole fraction evaporated. The procedure was repeated for the next time interval with the new droplet diameter and an adjusted mixture of components.

The first assumption in this approach is that there is sufficient internal mixing in the falling droplet to ensure a uniform distribution of the components, especially the more volatile hydrocarbons. It is important that this assumption be verified, for if there is little or no circulation then the evaporation rate will be much lower. In addition, the profile of the hydrocarbon vapors left in the atmosphere will be quite different. With adequate circulation in the droplets, the more volatile hydrocarbons would be deposited at the higher altitudes, whereas with no circulation there would be a more uniform distribution of all the hydrocarbons at all altitudes. Garner, et al. (Ref. 35) studied the internal circulation within falling droplets by taking colored motion pictures of organic liquid droplets containing anhydrous cobalt chloride falling through water. As the water diffused into the organic phase the cobalt chloride changed from deep blue to pink and thus acted as a tracer to define the internal flow patterns in the droplet. Under these conditions, internal circulation was observed at Reynolds numbers as low as 64 to 71 and it is inferred that it would occur at lower Reynolds numbers for liquids of lower viscosity.

To further check this assumption of droplet mixing, which would result in a fractioning evaporation of the free-falling JP-4 droplets, the following experiments were conducted.

6.1 EXPERIMENTAL APPARATUS

A closed-loop vertical wind tunnel was constructed as shown in Fig. 16. A variable-speed fan motor was used to set the airflow in the system. The air temperature was controlled by venting the boiloff gas from a liquid nitrogen supply through a cooling coil located below the fan. Air temperature was measured by a thermistor located in the upper horizontal leg of the loop. JP-4 droplets were formed by hypodermic needles located in the bottom of the reservoir, and the droplets fell down the vertical leg into a cooled collection sump. The evaporated hydrocarbon vapors were carried by the counterflow of air to the liquid-nitrogen-cooled cryopump located just above the fan. A thin-wall rubber septum was located by the side of the cryopump so that a sampling syringe could be inserted to collect the sample after a test sequence.

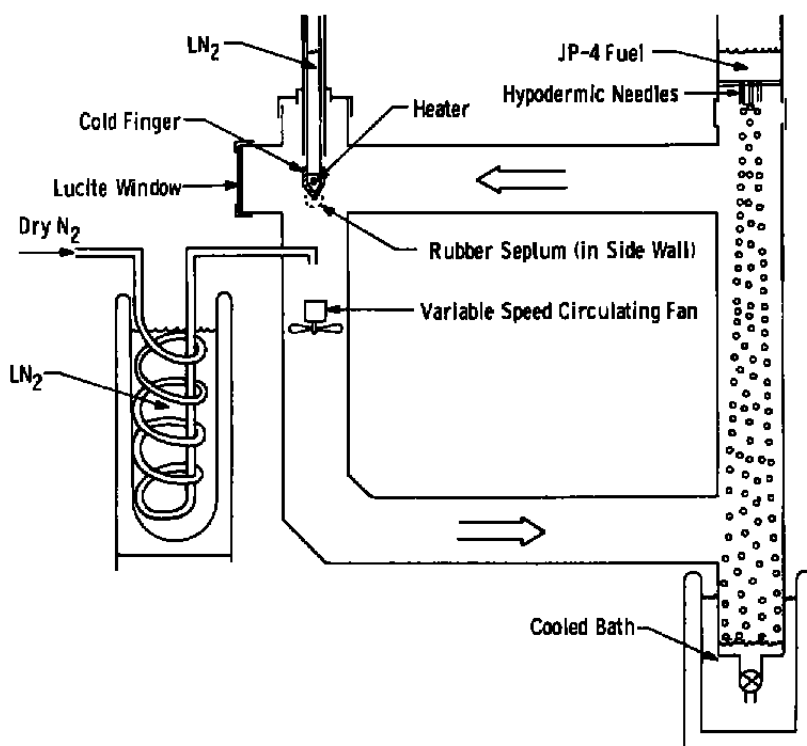


Figure 16. Schematic of closed-loop wind tunnel.

6.2 EXPERIMENTAL PROCEDURE

The system was first purged with dry nitrogen to remove as much water vapor as possible and then the fan speed was set and the cooling coils activated if the particular test sequence so required. When the airflow temperature had stabilized, liquid nitrogen was added to the cryopump. After it had cooled to 77°K, JP-4 was added to the reservoir (for some runs this JP-4 was precooled) and the droplets allowed to fall through the airstream. The droplets were allowed to fall for approximately two minutes and then the airflow was stopped. The heater in the cryopump was then turned on until the hydrocarbon cryofrost which had collected on its surface melted and formed a small droplet at its tip. The needle of the sampling syringe was then inserted through the septum and the droplet was collected for analysis. The sample size was typically 0.5 μ l.

6.3 ANALYSIS OF EVAPORATED COMPONENTS OF JP-4

Gas chromatography was used to analyze the evaporated components of the JP-4. Due to the large number of hydrocarbons present in JP-4, it was beyond the scope of this project to identify specific compounds and to quantify their concentration in the original JP-4 and the evaporated sample. The gas chromatograph was used to produce a fingerprint or signature of a particular sample so that it could be compared against a set of prepared fractions of JP-4.

The first part of this study was to find a suitable column for the gas chromatograph which would provide an acceptable separation of the hydrocarbon group. A standard packed column with SE30 was used initially since this was an accepted column for hydrocarbons. However, it was found that this column provided insufficient resolution of the early peaks. Schwartz, et al. (Ref. 36) reported good separation of complex hydrocarbon mixtures using a 200-ft capillary column coated with a mixture of hexadecene, hexadecane, and Kel-F[®] polymer oil. Such a column was procured from the Perkin Elmer Company and used for these tests. After investigating the many variables in the operating modes of the gas chromatograph, the following parameters were chosen as best suited for our particular application:

- a. Column - 200-ft by 0.01-in. capillary column coated with hexadecene, hexadecane and Kel-F,

- b. Detector - flame ionization,
- c. Oven temperature - constant 25°C,
- d. Carrier gas - N₂,
- e. Flow rate - 24 ml/min,
- f. Sample size - 0.5 μ l, and
- g. Injection - Hamilton constant pressure syringe.

6.4 CALIBRATION OF THE GAS CHROMATOGRAPH

The calibration of the gas chromatograph consisted of preparing a baseline chromatograph of the JP-4. One-hundred ml of this JP-4 was then distilled using the ASTM D86-1P 123 procedure (Ref. 37) and collected as twelve fractions. The data from this distillation along with the measured refractive index of each fraction are included in Table 4.

Table 4. Properties of JP-4 Fractions

Fraction No.	Volume, percent	Temperature, °C	Refractive Index
1	9	112	1.4074
2	9	124	1.4153
3	9	134	1.4179
4	9	144	1.4221
5	9	153	1.4263
6	9	168	1.4310
7	9	176	1.4357
8	9	186	1.4414
9	9	191	1.4460
10	9	198	1.4511
11	7	204	1.4574
12	3	Residue	1.4610

The temperature recorded in this method is that of the vapor at the head of the distillation column at the time that the noted percentage has been recovered. An analysis for percent olefins and aromatics was performed for the first four fractions and is included in Table 5. The gas chromatograms for these four fractions along with JP-4 is shown in Fig. 17. Only the first thirty minutes have been reproduced as being significant for this phase of the work, although the JP-4 data continue with over an additional 100 peaks. Markers have been included in Fig. 17 to identify the retention times of specific compounds.

The most volatile fraction was further subdivided by distillation into one-milliliter samples. Gas chromatograms of the first four of these samples are presented in Fig. 18.

Typical gas chromatograms obtained as "fingerprints" from the collected vapors off the cryopump from the closed-loop wind tunnel are shown in Fig. 19.

Table 5. Analysis of JP-4 fractions

Fraction No.	Volume, percent olefins	Volume, percent aromatics	Volume, percent saturates
1	0.44	4.95	94.61
2	0.57	7.43	92.00
3	0.65	9.10	90.25
4	0.71	10.95	88.34
JP-4	0.44	13.25	86.31

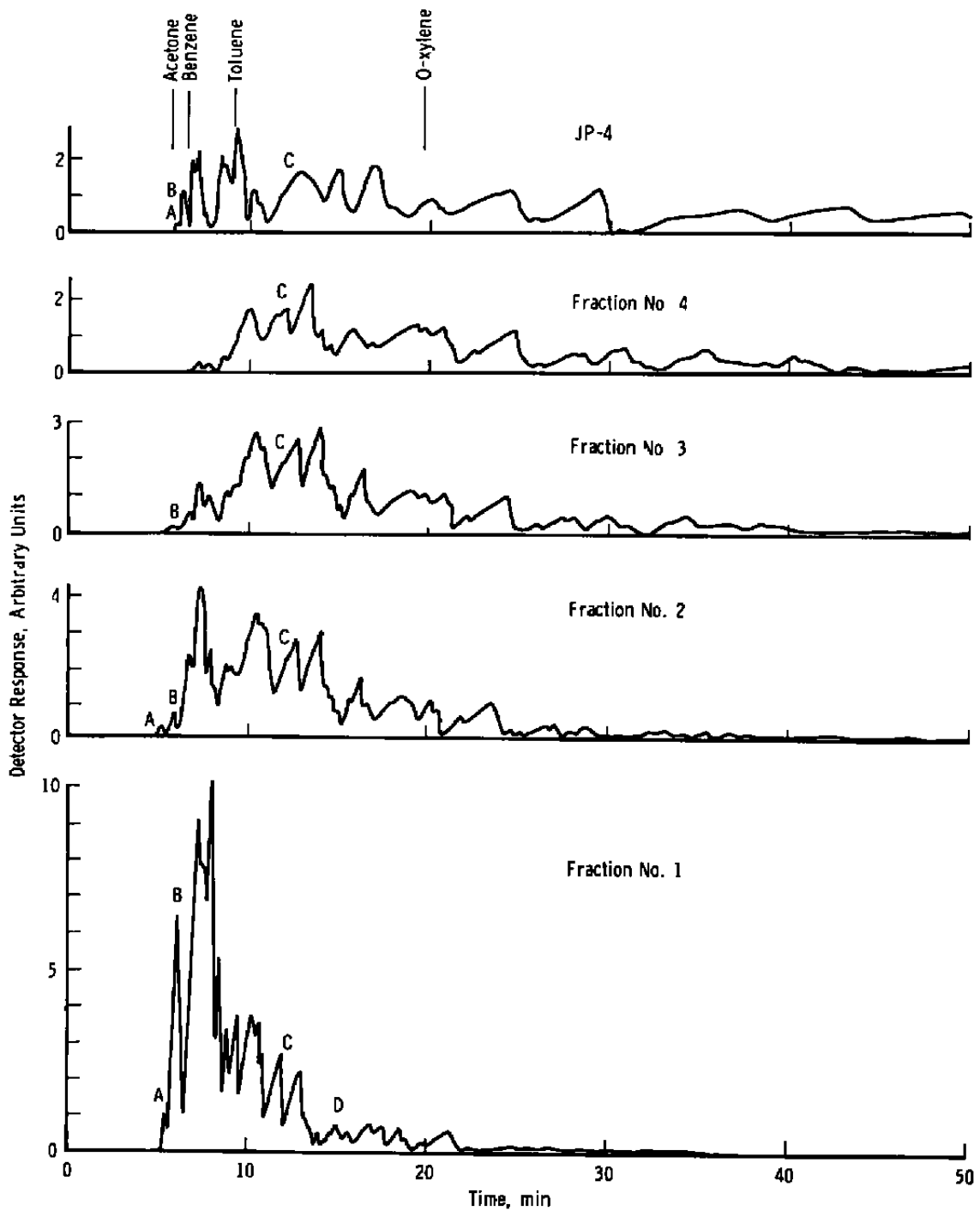


Figure 17. Gas chromatograms of JP-4 and fractions.

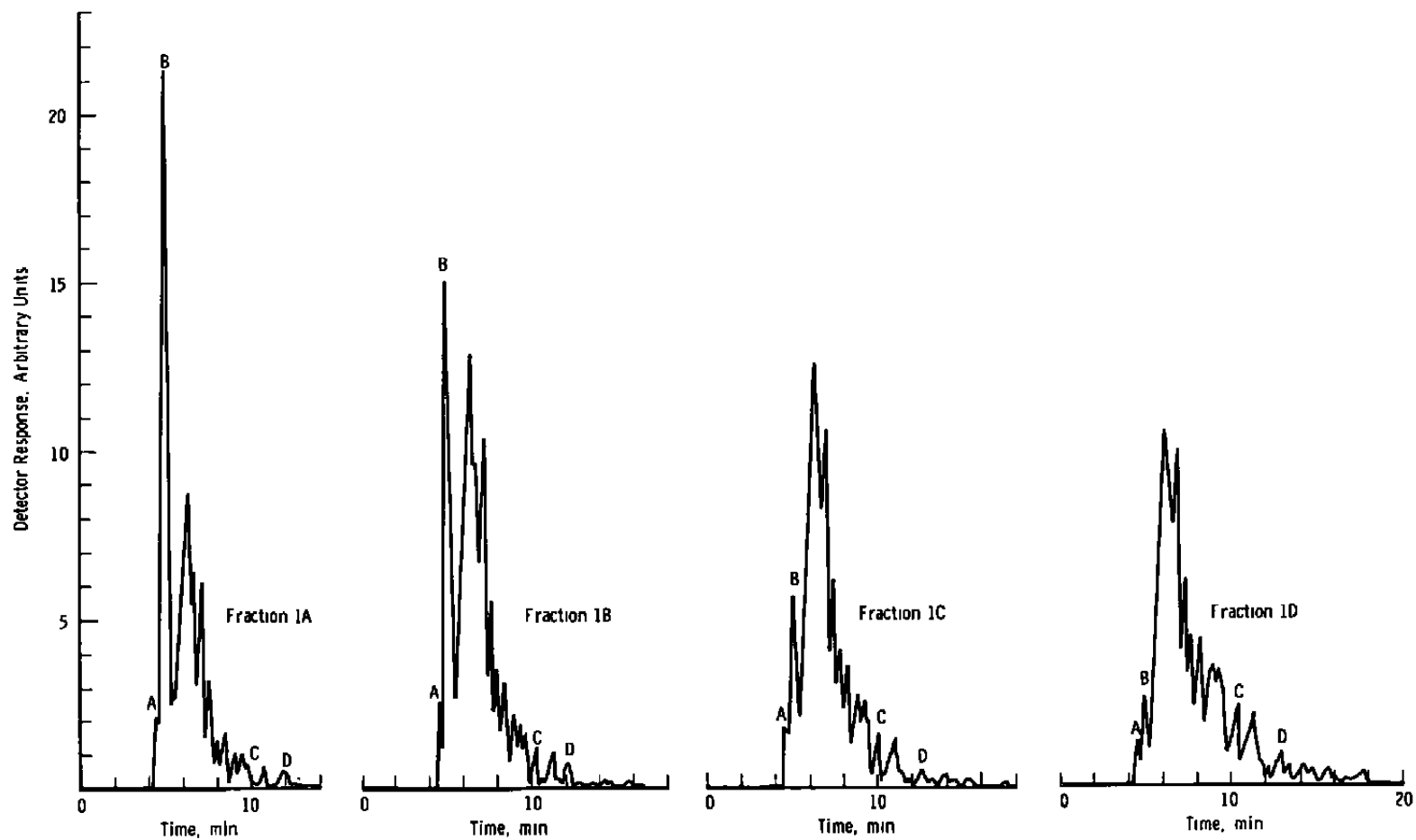


Figure 18. Gas chromatograms of 1-ml fractions.

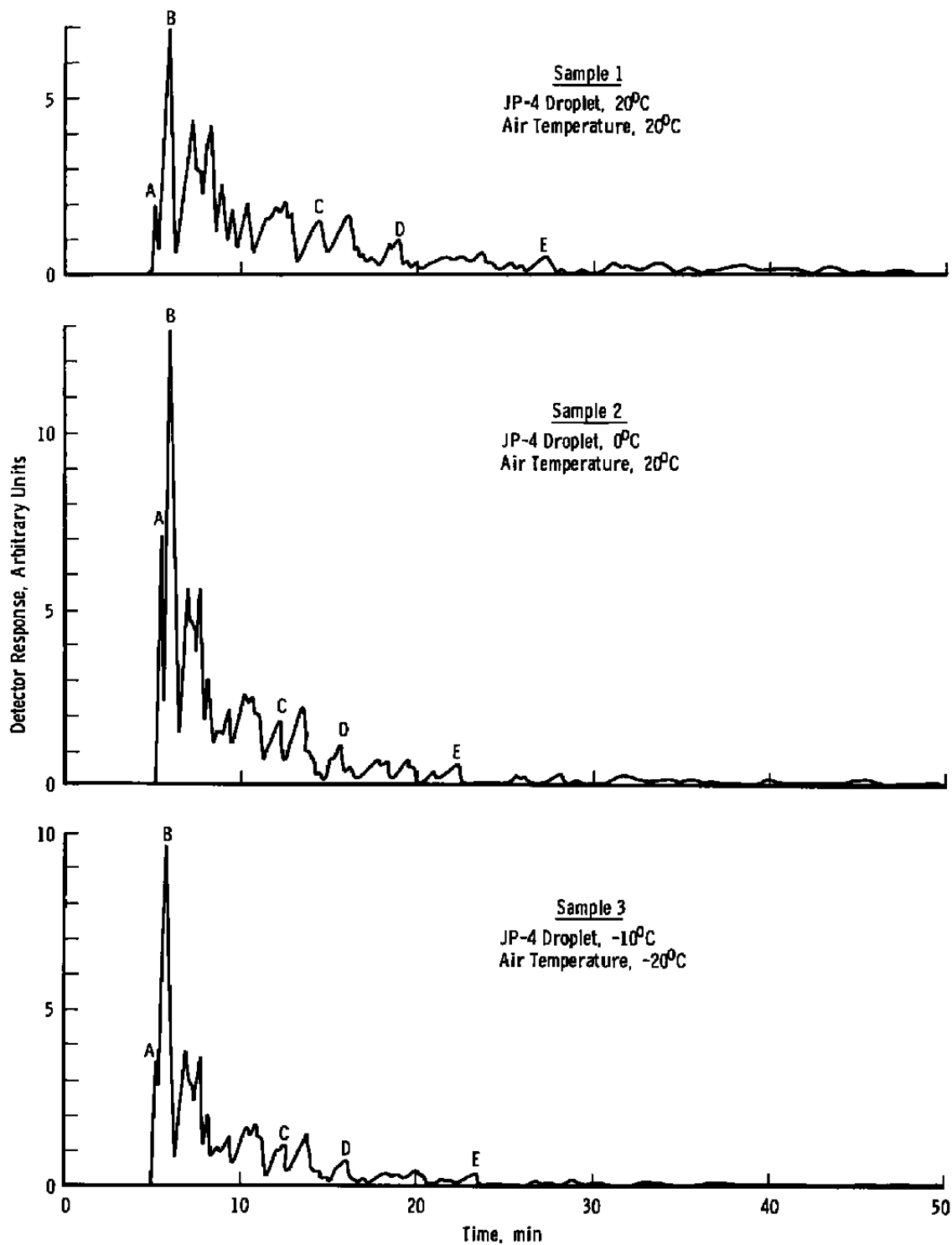


Figure 19. Typical chromatograms of evaporation samples.

6.5 DISCUSSION

All the gas chromatograms presented were prepared with a 0.5- μ l sample. The detector sensitivity and chart speeds were held constant, and thus all of the traces can be directly compared. The ordinate is presented as arbitrary units, although the relative concentration of the hydrocarbons represented by a specific peak, common to each chromatogram, is proportional to the area under that peak. Sequential peaks in a chromatogram, however, cannot be so easily compared. The response of the flame ionization detector to pure hydrocarbons (containing only hydrogen and carbon) is approximately linear with respect to carbon number; however, substituted groups (halogen, sulphur, oxygen, nitrogen, etc.) decrease the sensitivity. Thus, the flame ionization detector requires calibration with known compounds for quantitative analysis. For these studies, however, it is sufficient to note that with a constant-volume sample a general increase in one section of the chromatogram indicates an increase in abundance of these species and must result in a general decrease in the other parts of the chromatogram. This is quite evident when comparing JP-4 to the fractions in Fig. 17. The more volatile components represented by peaks A and B are quite evident in fraction No. 1 but are barely discernible in JP-4.

The retention time, or separation between peaks, can vary slightly from day to day due to slight differences in setting the carrier gas flow rate. This effect can be seen by comparing peaks, A, B, C, D, and E on the curves in Fig. 19. The general character of the peaks are retained and are identifiable which is sufficient for these tests. These data indicate that there is very little difference in the composition of the evaporated species as a result of varying the droplet temperature or the air temperature. Comparing the ratio of peak B with the following doublet peak in both samples 1 and 2 indicates a slight decrease of the more volatile components in favor of the later components for the higher droplet temperature. A similar examination of samples 2 and 3 indicates that these samples are indistinguishable. The apparent overall, slightly lower signal level coefficient is most likely due to the inclusion of a small bubble in the hypodermic needle and thus the injection of a slightly smaller sample into the gas chromatograph.

When comparing the evaporation samples against the fractions (Fig. 18) it is obvious that they fall close to fraction No. 1A. This fraction represents the most volatile components of JP-4 and is one percent by volume of the whole JP-4. It should also be noted that a small percentage of each evaporation sample contains species beyond peak D

which are not evident in fraction No. 1A. This is to be expected since fraction No. 1A is the result of a double distillation process designed to remove the less volatile components.

Subsequent experiments to determine droplet evaporation rates (see Section 7.0) indicate that in these tests approximately 0.8 percent by volume of the droplets evaporated in the free fall. This suggests, therefore, that the bulk of the more volatile species are evaporating during the early part of the free fall, and the assumption of adequate internal mixing is valid.

7.0 EVAPORATION RATES OF JP-4 DROPLETS

In order to predict the distribution of hydrocarbon vapors in the atmosphere from a particular fuel dump, it will be necessary to develop a computer program similar to that devised by Lowell (Refs. 32 and 33). His work was limited by the capacity and ability of the computers available to him at that time. Unfortunately, there are no readily available experimental data to check his calculations against. Realizing the need for some evaporation rate data for JP-4 droplets in moving airstreams which might be used for checking the validity of a future computer code, the following experiments were planned and executed.

The method used was similar to that developed by Frossling (Ref. 29) and consisted of suspending a droplet of JP-4 on a fine glass filament in a conditioned airstream. Droplet sizes were determined from a sequence of photographs taken of the droplet as it evaporated.

7.1 EXPERIMENTAL APPARATUS

The experimental apparatus to study the evaporation rate of JP-4 droplets is shown in Fig. 20. It consisted of a plexiglass test section, motor-driven sequence camera with strong flash light, a multimeter readout for temperature probes, and a micromanometer used to measure pitot tube pressures. Details of the test section are shown in Fig. 21.

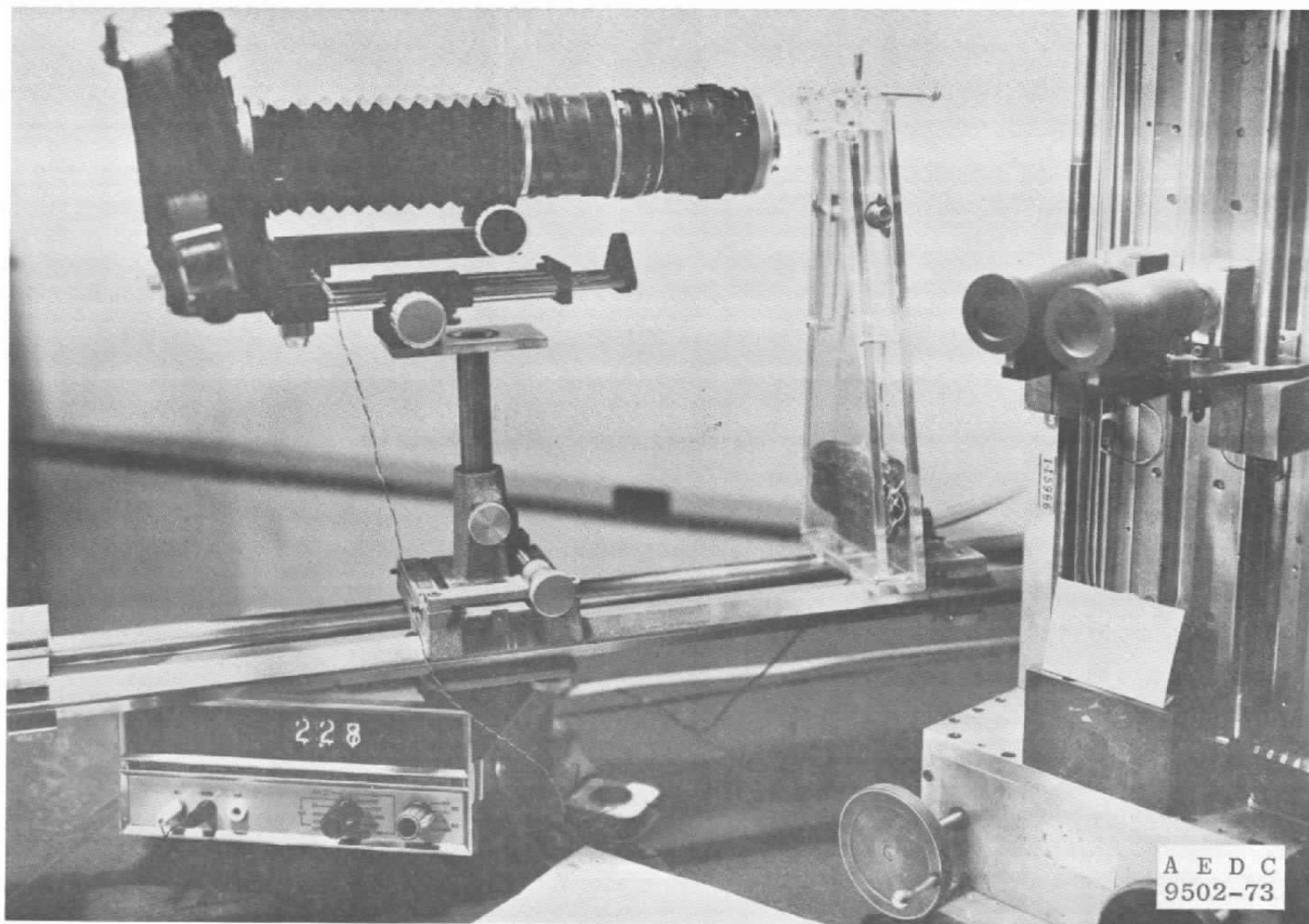


Figure 20. Pendant drop test apparatus.

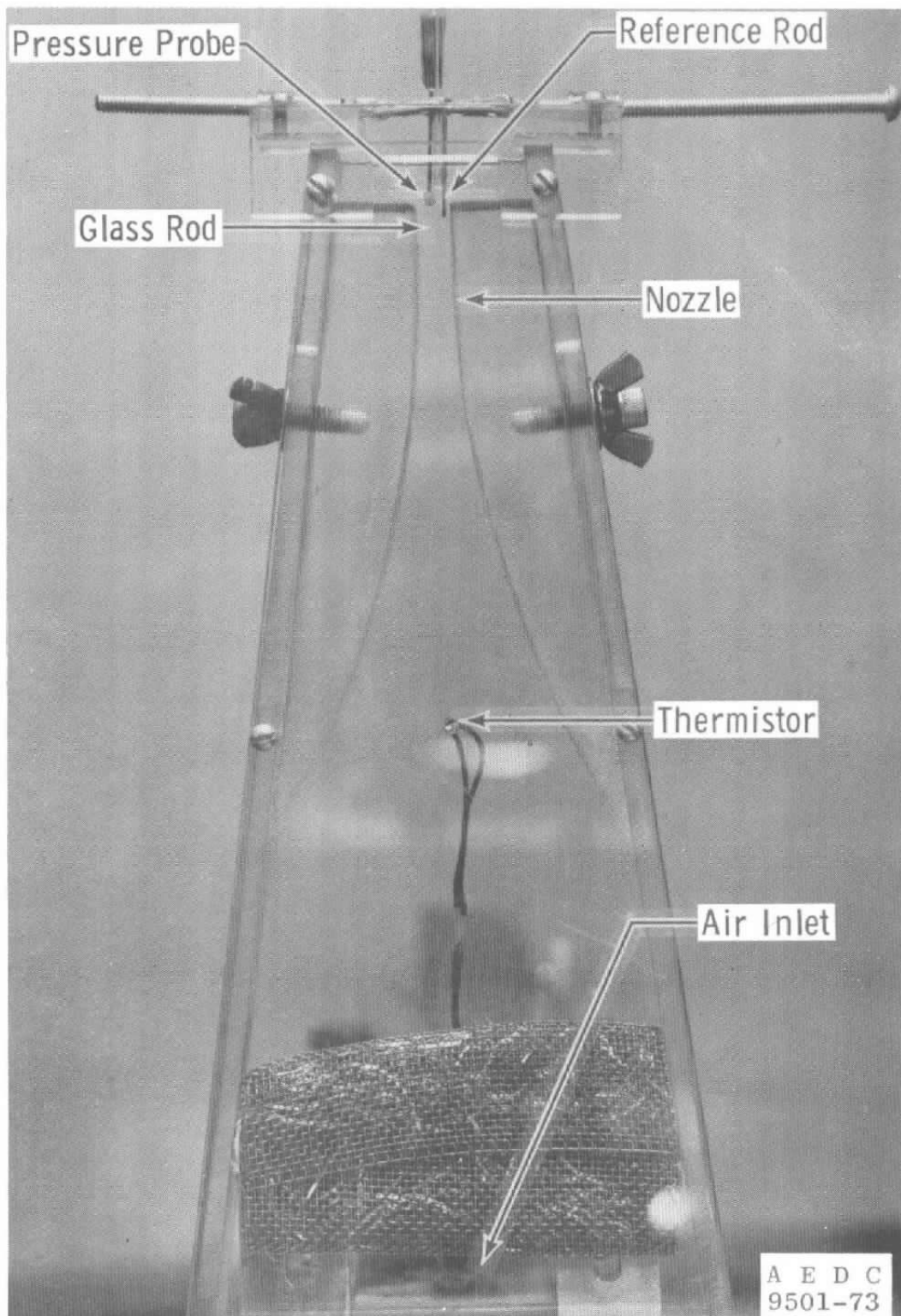


Figure 21. Drop support and adjustable nozzle.

The airstream entered at the base and was then directed through a section of wire mesh and aluminum turnings to dampen turbulence. The airstream temperature was measured by a thermistor just as it entered the adjustable nozzle section. The air temperature was controlled by passing the air supply through a copper coil which could be partially immersed in a bath of liquid nitrogen. The required temperature in the test section was adjusted by increasing or decreasing the number of turns of the copper coil which were immersed in the liquid. The humidity was adjusted by passing part of the flow through a canister filled with wet cotton fibers. The velocity of the airflow around the droplet was controlled by adjusting the throat cross-sectional area and regulating the air supply pressure. The air velocity was determined by measuring the stagnation pressure with a pitot probe, shown in Fig. 21, with the spherical tip. The rod located to the right of the pitot probe was located in the same photographic plane as the suspended JP-4 droplet and was used as the reference dimension in all of the droplet photographs. The glass filament (138- μ m-diam) barely visible in Fig. 21 is shown enlarged in Fig. 22 along with a JP-4 droplet.

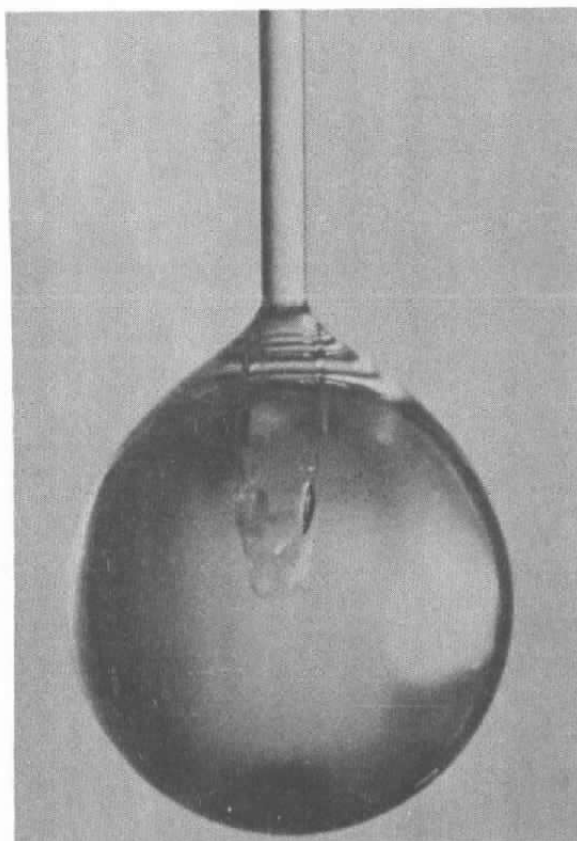


Figure 22. JP-4 droplet on glass filament.

The photographs were taken with a 50-mm lens using bellows and extender rings to produce a 5.3X magnification of the droplet at the negative. This negative was further enlarged on the film reader used to recover the data. The timing sequence was set by an intervalometer which automatically triggered the camera. Illumination was supplied by an electronic strobe flash unit, and the light was diffusely reflected from a white screen background.

7.2 EXPERIMENTAL PROCEDURE

Prior to suspending the droplet of JP-4 on the glass rod, the desired flow conditions were established by adjusting the test section throat and the air supply pressure. For those runs requiring temperature or humidity control, the appropriate conditioning systems were installed in the air supply line. After the camera system was set and focused, the airflow was momentarily interrupted by disconnecting the supply line to the test section, and the droplet was transferred to the glass support rod from a pipette made from a fine drawn glass tube. The air supply was immediately reconnected and the intervalometer started.

7.3 DATA REDUCTION

Observation of the suspended droplets during checkout runs indicated that their shape deviated from a true sphere due to their contact with the glass support rod as well as to aerodynamic forces. An extreme of this distortion is shown in Fig. 23 which is one of the last frames of an evaporation sequence. The air velocity is 3.05 m/sec, and as can be quite easily seen it has driven the droplet well up the glass support rod.

Several photographs of droplets were mapped using a Benson-Lehner Telereader®. This system projected a 20X magnified image from the negative, and a drivable set of cross hairs could be located at any point. Upon command, the coordinates were automatically recorded and punched on computer cards. Figure 24 presents a typical map of a droplet along with the best fit ellipse. Assuming that the droplets are symmetrical about their major axis, their volumes were calculated from the best-fit prolate spheroid. An equivalent droplet diameter (d_0) was defined as a spherical droplet with the same volume.

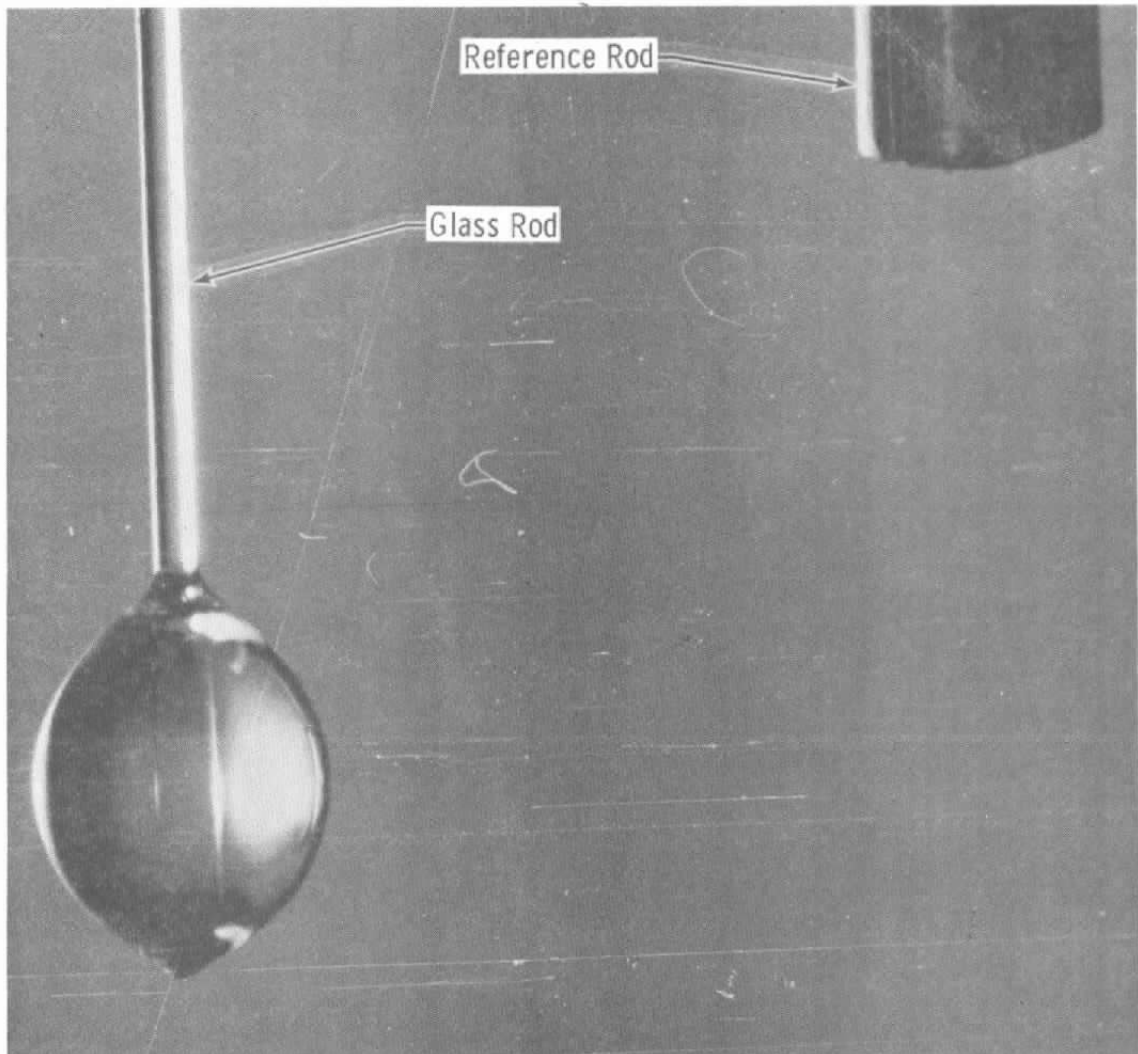


Figure 23. Evaporating droplet on sting.

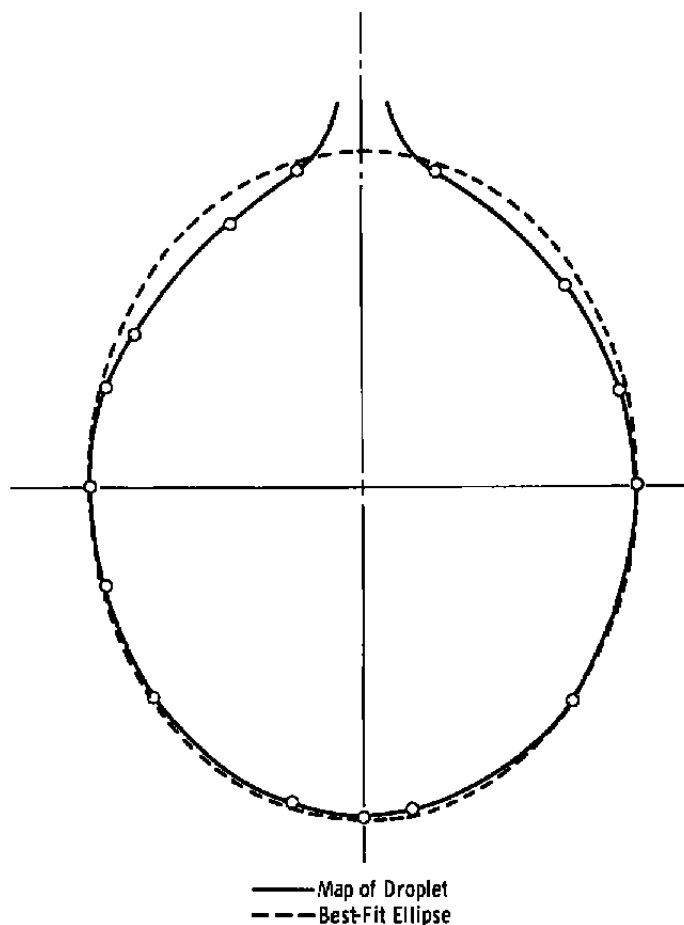


Figure 24. Map of suspended droplet.

Assuming that the evaporation rate for a pure liquid droplet suspended in an airstream is directly proportional to the surface area, then

$$-\frac{dm}{dt} = C^*[A_s] \quad (5)$$

where

$$\frac{dm}{dt} = \text{evaporation rate (gm/sec)}$$

$$C^* = \text{constant (gm/sec-cm}^2\text{)}$$

$$A = \text{surface area of droplet, cm}^2$$

The surface area of a prolate spheroid is

$$A = \pi^2 \left[x^2 + \frac{xy}{\epsilon} \sin^{-1} \epsilon \right] \quad (6)$$

where

y = major axis, cm

x = minor axis, cm

and

$$\epsilon = \sqrt{\frac{y^2 - x^2}{y}}$$

The mass is given as

$$m = \frac{\pi}{6} (\rho) x^2 y$$

where

ρ = density (gm/cm³)

Thus,

$$\frac{dm}{dt} = \frac{\pi \rho}{6} \left(2yx \frac{dx}{dt} + x^2 \frac{dy}{dt} \right) \quad (7)$$

Substituting (6) and (7) in Eq. (5) and rearranging thus yields

$$C^* = -\frac{\rho}{3} \left[\frac{2y \frac{dx}{dt} + x \frac{dy}{dt}}{x + \frac{y}{\epsilon} \sin^{-1} \epsilon} \right] \quad (8)$$

Equations (7) and (8) were evaluated numerically using the time interval between successive photographs. The derivatives at $t = 0$ and $t = t_{\text{final}}$ were evaluated using the forward and backward difference approximation. An evaluation of C^* for both distilled water droplets and JP-4 is presented in Fig. 25.

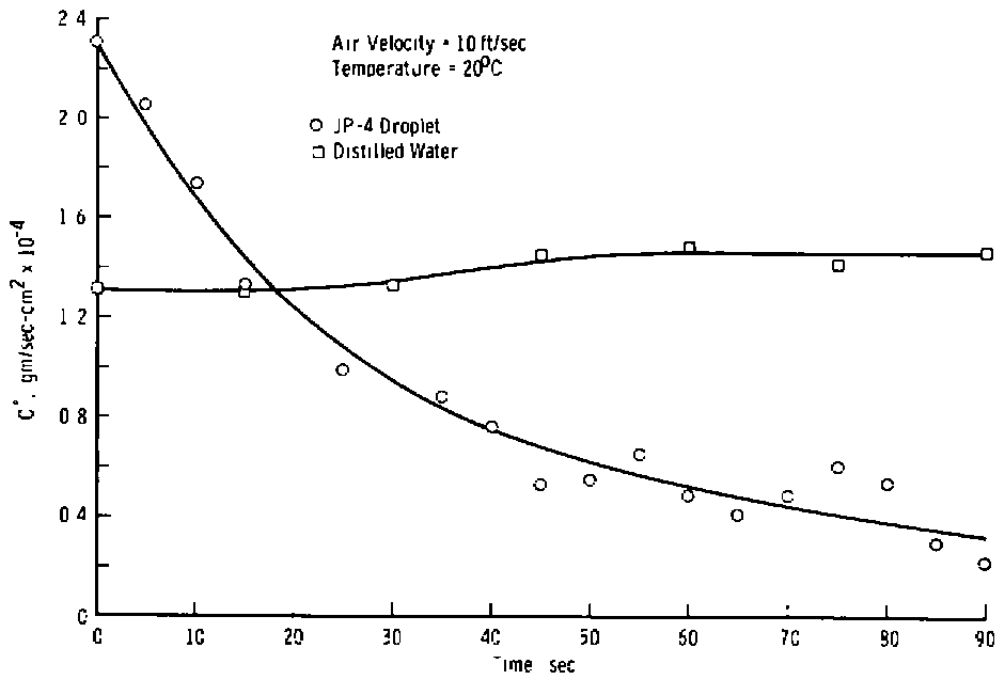


Figure 25. Evaporation rate as a function of time.

7.4 RESULTS

Using the previously described techniques, a series of tests was conducted. Several preliminary test runs were made in which a droplet of JP-4 was suspended on a small thermistor and hung in the test cell airstream. It was noted that even on those occasions where there were 3 or 4°C differences between the initial droplet temperature and the airstream (cooled airflows) the droplet quickly accommodated to the airstream temperature and remained constant within 0.2°C. This agrees with Frossling's observations (Ref. 29). In all further tests it was therefore assumed that the droplet temperature was that of the airstream. Data were obtained for the following range of parameters:

- Air velocity 0, 10, 15, and 20 ft/sec,
- Air temperature -25°C, -10°C, and 20°C at 10 ft/sec,
- Humidity 11, 27, 40, and 67 percent at 10 ft/sec, and
- Liquid droplet H₂O, JP-4, and JP-4 fractions.

It was found that it was quite difficult to suspend a predetermined specific drop size on the glass filament and so the first series of tests was made with the humidity, air temperature, and air velocity fixed, and the data were taken for a range of droplet sizes from 1060 to 1347 μm in diameter. The data are presented in Fig. 26. These curves collapse to a single curve when the evaporation rate is reduced to the effective evaporation rate from a 1000- μm droplet. Where

$$\frac{dM}{dt} \text{ (effective)} = \left(\frac{1000}{d_0} \right)^3 \frac{dM}{dt} \text{ (measured)}$$

and

$$d_0 = \text{initial equivalent droplet diameter } (\mu\text{m})$$

For these curves the mass was calculated using a constant density which is not strictly true, although it is considered adequate for these presentations.

A second set of experiments was conducted in which the air velocity and temperature were held constant, and the relative humidity was varied from 11 to 67 percent. These data were once again reduced to indicate the evaporation rate of an effective droplet of 1000- μm diameter and are presented in Fig. 27. The spread can be considered as a result of experimental uncertainties and thus indicates no apparent effect on the evaporation rate due to the relative humidity of the ambient air.

The third series of experiments was conducted with the air temperature held constant and the air velocity varied from 0 to 20 ft/sec. The curves presented in Fig. 28 are averaged from data taken for several drop sizes at each air velocity. Once again, they have been reduced to an effective 1000- μm droplet. A crossplot of this data presented in Fig. 29 indicates that the evaporation rates measured were a direct function of the air velocity.

Several problems were encountered in making the experimental runs at reduced temperatures. The prime trouble was in obtaining sharply focused photographs of the droplets. Dry nitrogen was used to purge the outside of the test section; however, the inside of the plexiglass windows gradually fogged up during the long run times necessary to establish a steady-state flow and then record the droplet evaporation. The data presented in Fig. 30 are representative of the runs made and may be useful for "ballpark" estimates. However, insufficient repetitive points were

obtained to provide any crossplots giving evaporation rates as a function of temperature.

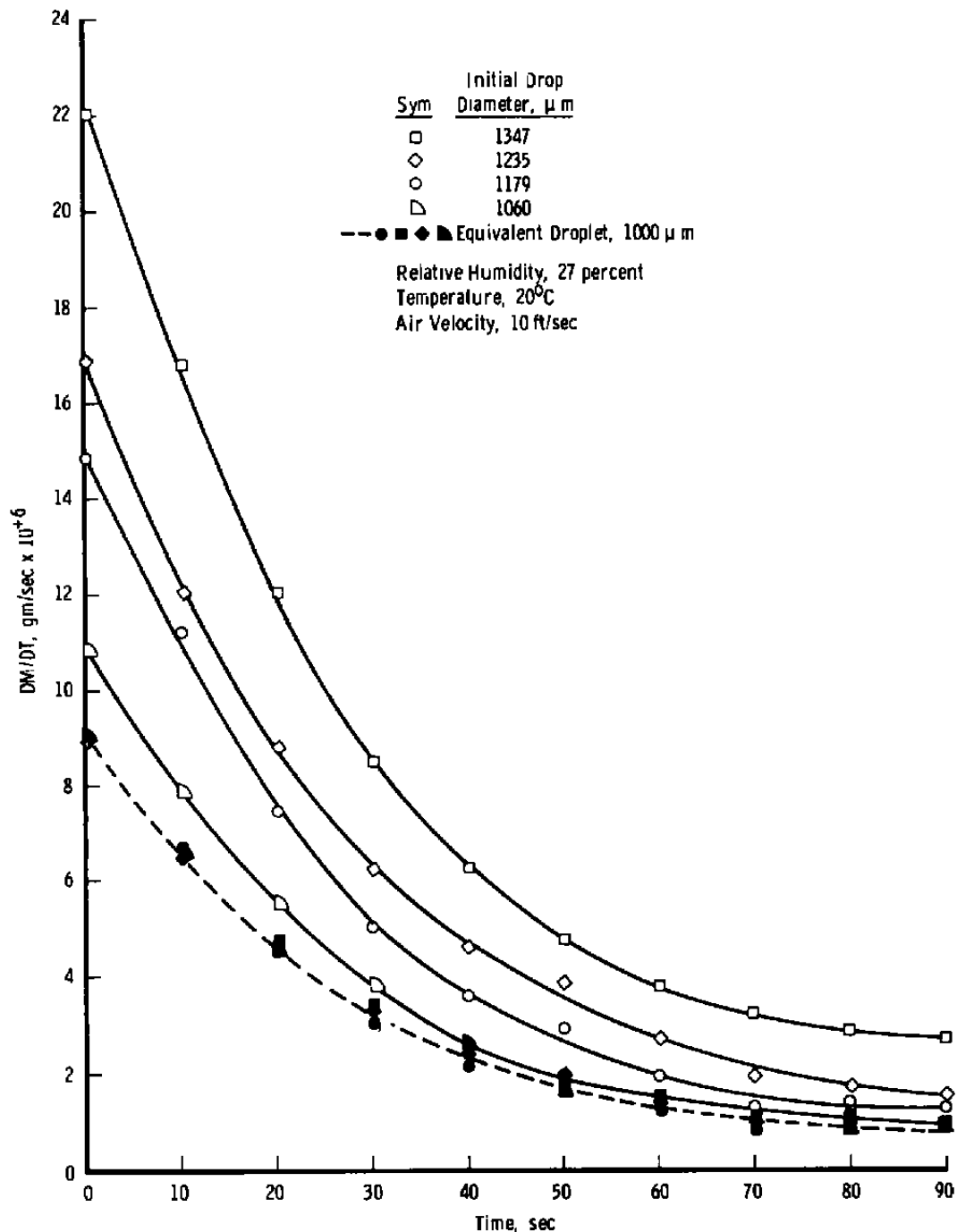


Figure 26. Evaporation rate of JP-4 droplets.

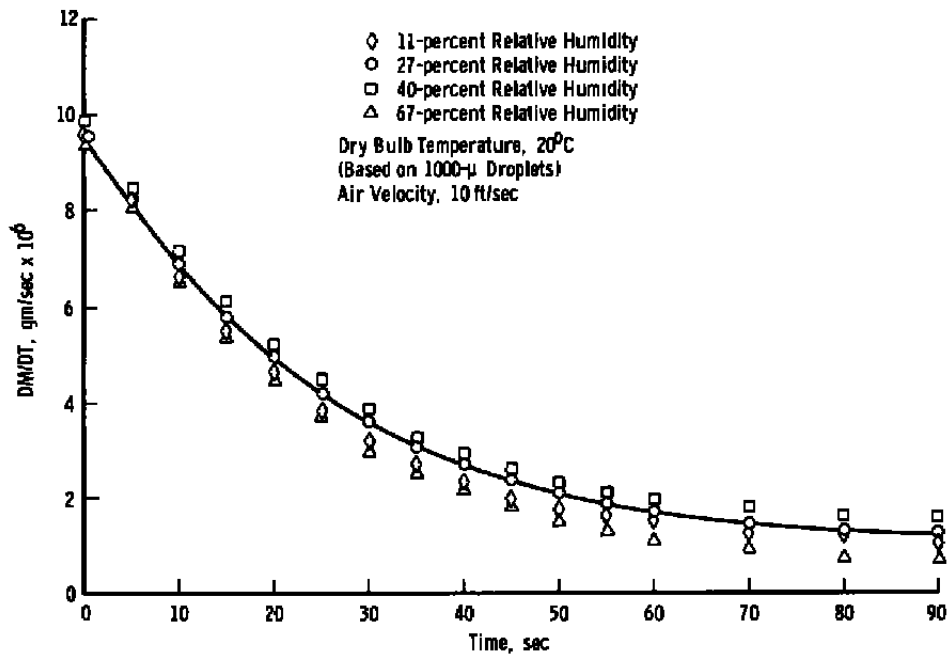


Figure 27. Evaporation rate of JP-4 at various humidities.

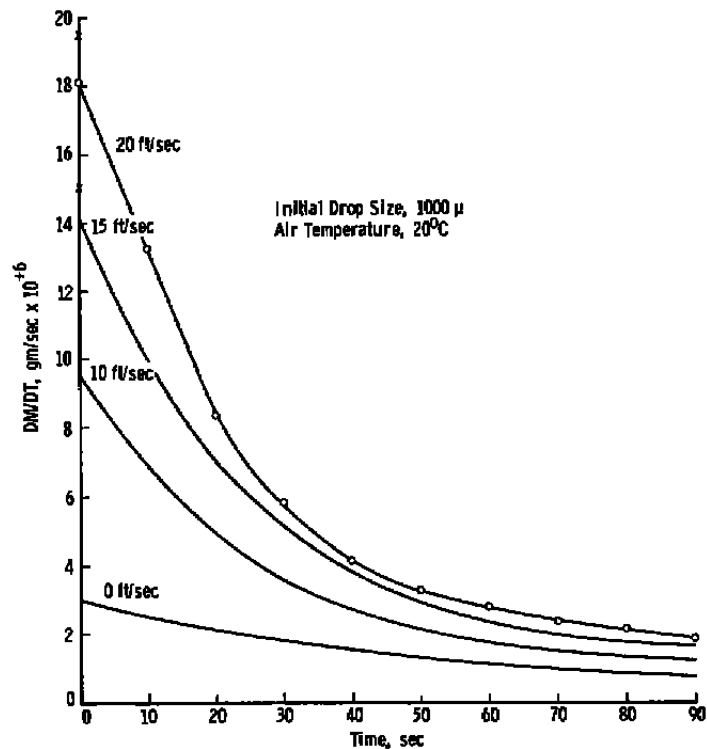


Figure 28. Evaporation rate of JP-4 for various air velocities.

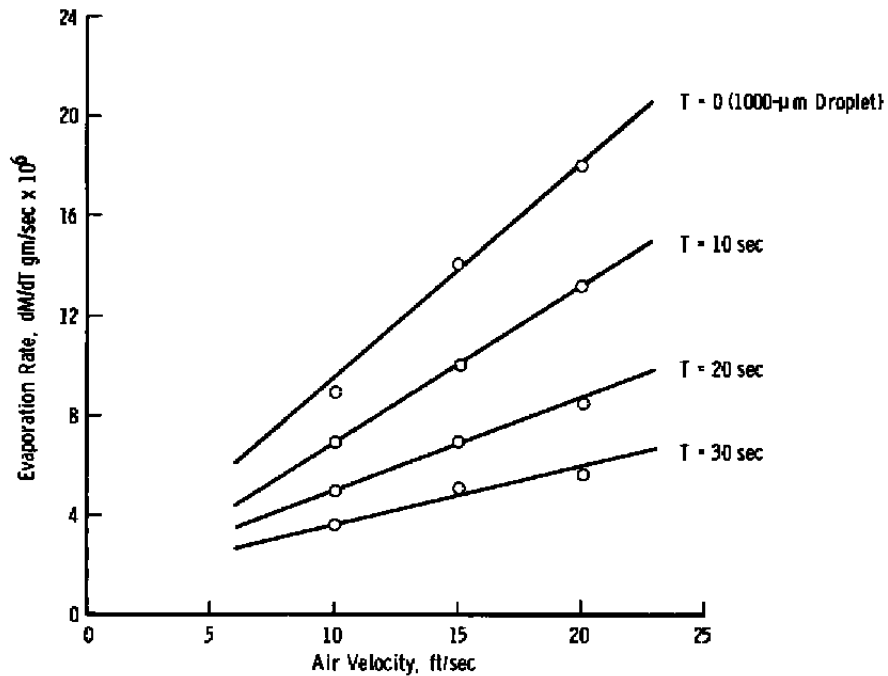


Figure 29. Evaporation rate versus air velocity.

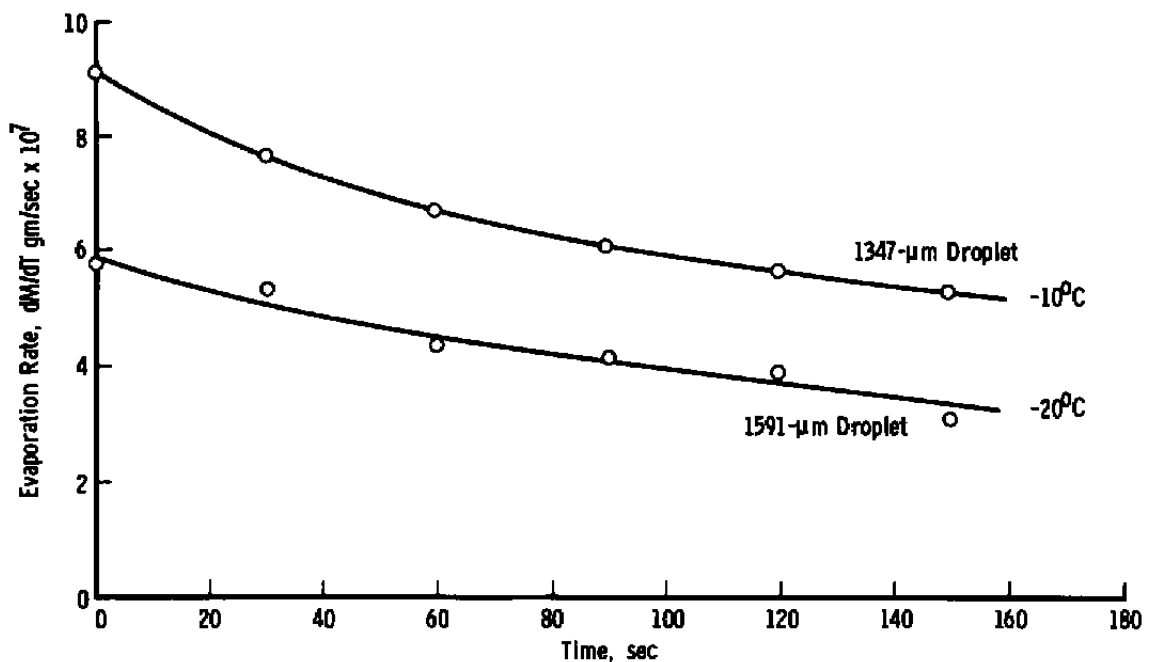


Figure 30. Evaporation of droplets in cooled airflows.

Several runs were made with droplets taken from the fractions of JP-4 recovered from the distillation system (see Table 4). Figure 31 is a presentation of the evaporation rates of four of the fractions. It is interesting to note from the data that the evaporation "constant" C^* for these fractions can be expressed as a direct function of time for the first 50 percent of the mass evaporated.

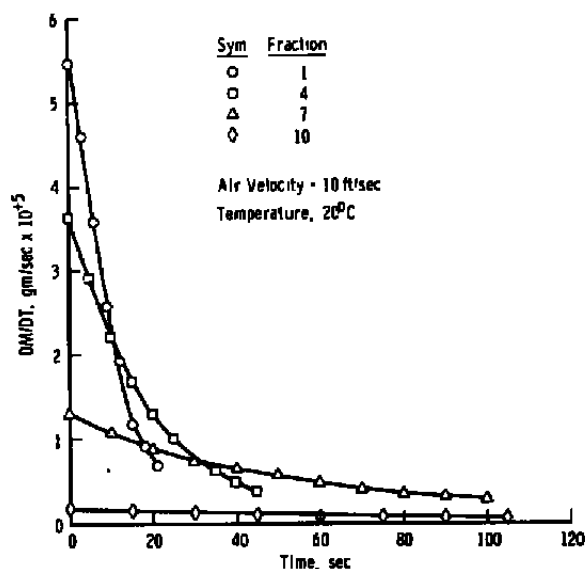


Figure 31. Evaporation rate of JP-4 fractions.

These values are represented by

$$C^* = (A + Bt)10^{-4} \text{ gm} \cdot \text{sec} \cdot \text{cm}^2$$

where the values of A and B are given in Table 6 and t is measured in seconds.

Table 6. Empirically Determined Constants for Evaporation Rate Equation

Fraction	A	B
1	1.45	3.9×10^{-2}
4	0.75	1.17×10^{-2}
7	0.23	1.75×10^{-3}
10	0.04	3.67×10^{-4}

8.0 VAPOR PRESSURE OF JP-4 AND RESIDUALS

In order to provide some experimental data on the vapor pressure of a cooled evaporating droplet, a series of tests was performed using a small sample (approximately 5 ml) of JP-4.

8.1 EXPERIMENTAL APPARATUS

A schematic of the apparatus is shown in Fig. 32. The sample tube was fitted with a calibrated thermistor to measure temperature and a transducer to determine the pressure. The vacuum pump was used to both purge the air from the system and to remove the vapors as the sample was slowly evaporating between data points. The sample holder was supported such that it could be completely immersed in a cooled bath of ethylene glycol and dry ice.

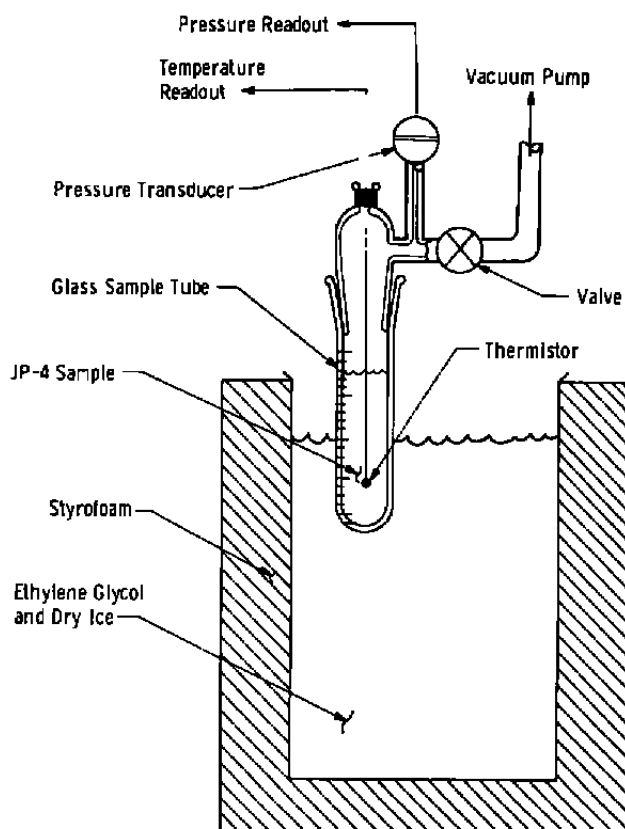


Figure 32. Schematic of apparatus used to measure vapor pressure.

8.2 EXPERIMENTAL PROCEDURE

A sample of JP-4 was introduced into the test tube and the system was sealed. The tube was then immersed in the cold bath and cooled to -60°C . When it had reached this temperature, the valve to the vacuum pump was opened and the pressure reduced to below one millimeter of mercury. The valve was then closed and the system was allowed to stabilize. When the temperature and the pressure had reached a steady state, the pressure and temperature were recorded, and the cold bath was warmed slightly. This process was repeated until the JP-4 was returned to room temperature. The valve to the vacuum pump was then opened and left open until 10 percent of the JP-4 had evaporated. At this point, the valve was closed and the test volume again cooled with the cold bath. Again, data were obtained for the vapor pressure of the 90-percent residual. This process was repeated with 0.5 ml of the sample being evaporated between successive runs.

A plot of vapor pressure versus temperature for JP-4 and the various residuals is presented in Fig. 33.

8.3 DISCUSSION

The evaporation process in this experiment does not duplicate that of a ventilated droplet; however, it was noted that during the pumpout period there were significant convection currents in the bulk of the liquid sample. This would indicate that as in the falling droplet there was sufficient mixing occurring to allow the more volatile components to move to the surface. As can be seen in Fig. 33, the vapor pressure follows the $\log 1/T$ relationship except for a slight deviation at the lower pressures. After observing this deviation, the thermistor and the pressure transducer were checked in situ, the thermistor against a mercury thermometer and the transducer against a calibrated aneroid-type pressure gage. It was decided that neither of these measurements could be the source of the deviation. During the period that these data were taken, it was therefore considered that this was a real deviation due to the complex mixture of hydrocarbons in JP-4. However, it has since been suggested that this may have been due to an adsorption of some of the high vapor pressure hydrocarbons by the elastomer seat in the vacuum valve used to isolate the vacuum pump. Thus, at the lower temperatures these components were adsorbed and then desorbed as the temperature was raised.

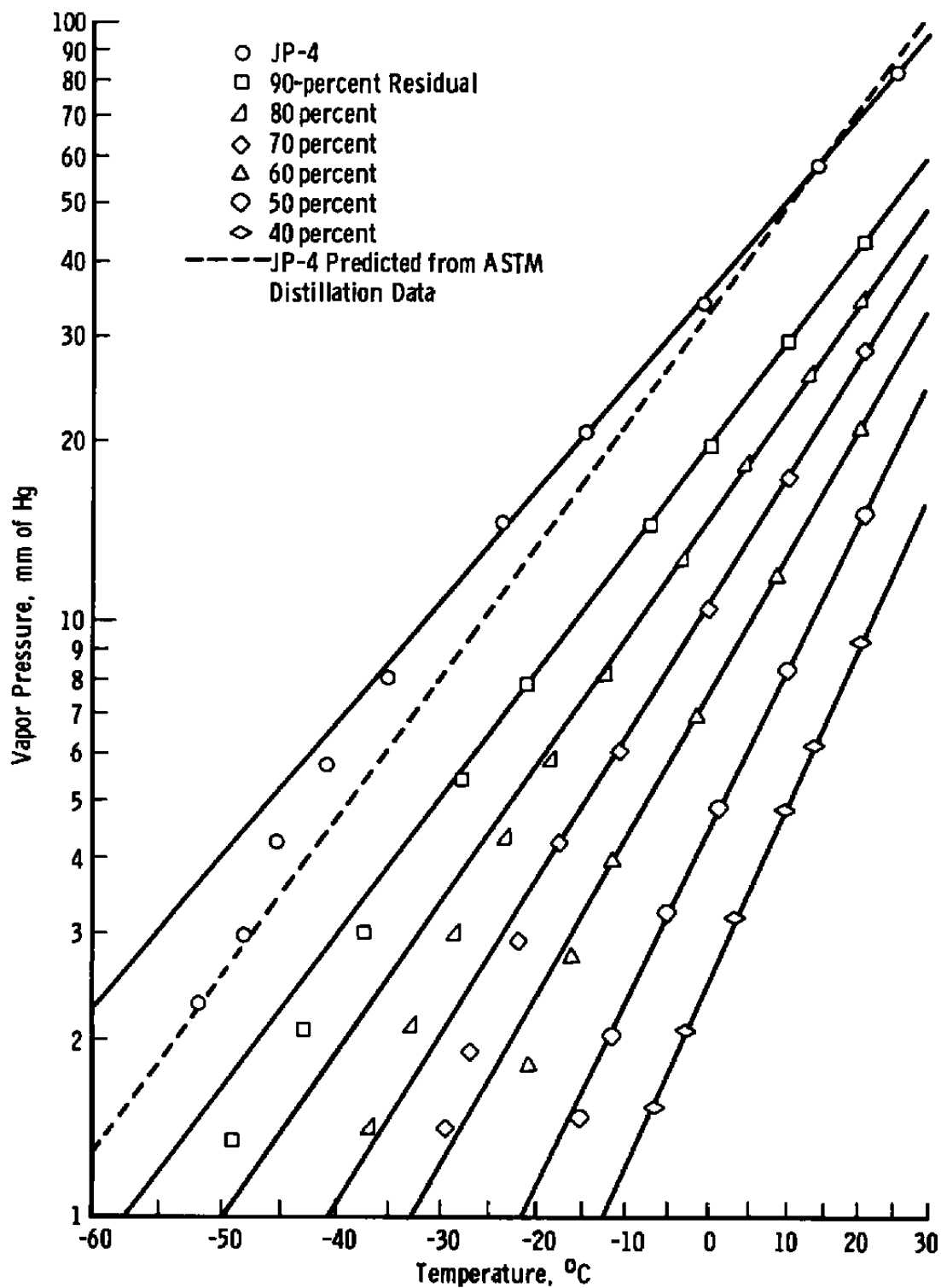


Figure 33. Vapor pressure of JP-4 and residuals.

It should be noted however that the data presented are for a specific sample of JP-4. They are therefore useful only insofar as they give guideline information on what are reasonable assumptions which may be made in developing a tractable computer model to describe the evaporation process.

9.0 EFFECTS OF JP-4 ON CONDENSATION OF ATMOSPHERIC WATER VAPOR

In order to study the effects of fuel vapors on the condensation of water on naturally occurring condensation nuclei, a Wilson-type cloud chamber (Fig. 34) was constructed. This system was chosen in favor of the simpler diffusion-type cloud chamber because it is better suited for adding contaminants and it can be cycled to both condense and re-evaporate the water droplets. Therefore, it can more realistically reproduce the life cycle of a small droplet involved in a dynamic cloud environment.

The condensation process is initiated by slightly cooling the test volume of the cloud chamber which contains the particulates and vapors to be investigated. This cooling is accomplished by a slight adiabatic expansion produced by a large piston.

The supersaturation produced in a given expansion of the chamber is calculated using the initial temperature and the initial and final pressures. The pressure data are used to determine the final temperature rather than attempting to measure the temperature directly because of the inherent thermal lag in any temperature-measuring device. This temperature is calculated from the adiabatic relationship

$$T_2 = T_1 \left(\frac{P_1}{P_2} \right)^{\frac{1-\gamma_{eff}}{\gamma_{eff}}}$$

where γ_{eff} is an effective ratio of specific heats of the air and water vapor and is given by Richarz (Ref. 38) as

$$\left(\frac{1}{\gamma_{eff}-1} \right) = \left(\frac{1}{\gamma_{air}-1} \right) \frac{P_{air}}{P_{total}} + \left(\frac{1}{\gamma_{water\ vapor}-1} \right) \frac{P_{water\ vapor}}{P_{total}}$$

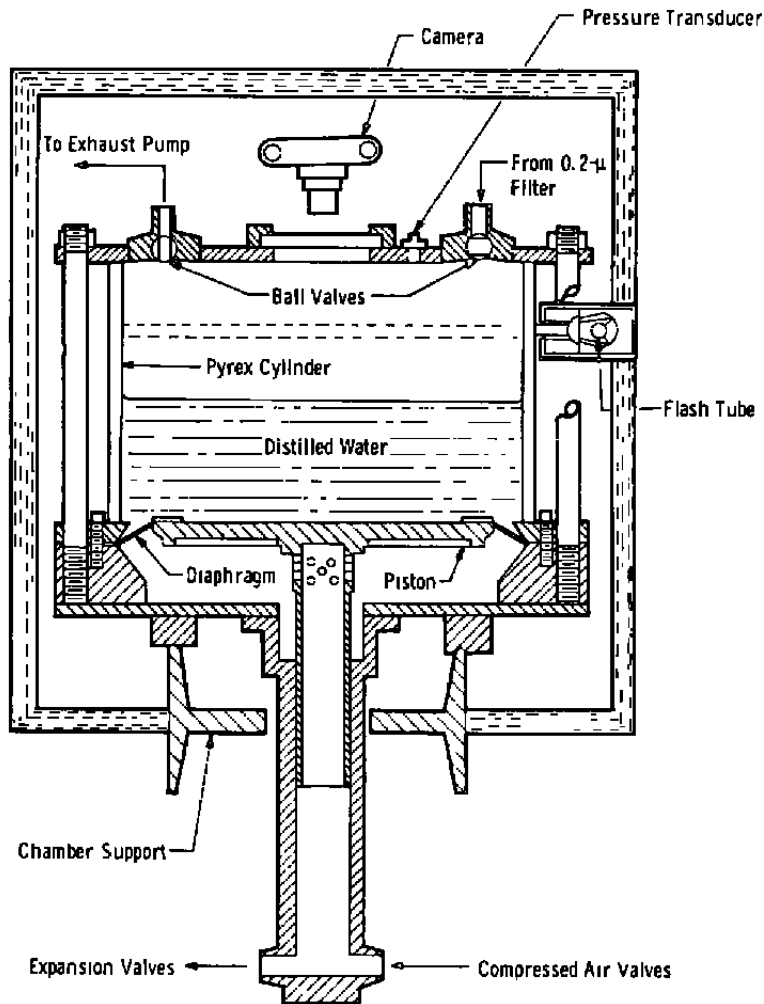


Figure 34. Schematic of cloud chamber.

The supersaturation is defined as

$$S = \frac{\rho}{\rho_{\infty}}$$

where

ρ is the actual vapor density

and

ρ_{∞} is the equilibrium vapor density of the vapor over a plane surface of the liquid phase

Assuming a closed system at initial conditions, P_1 , V_1 , and T_1 which undergoes adiabatic expansion, the temperature and pressure are lowered to T_2 , P_2 , and the volume increases to V_2 . Assuming that there is no condensation during this rapid expansion, then the number of vapor molecules remains constant. The final vapor density is therefore

$$\rho_2 = \rho_1 \left(\frac{V_1}{V_2} \right)$$

or

$$\rho_2 = \frac{P_{v1}}{RT_1} \left(\frac{V_1}{V_2} \right)$$

where P_{v1} is the initial pressure of the water vapor which was in equilibrium with the surface of the liquid phase in the chamber at the temperature T_1 . The density of water vapor for equilibrium at the final temperature T_2 can similarly be written as

$$\rho_\infty = \frac{P_{v2}}{RT_2}$$

Thus, the supersaturation may be rewritten as

$$S = \frac{\rho_2}{\rho_\infty} = \frac{P_{v1}}{P_{v2}} \left(\frac{P_2}{P_1} \right)$$

In the absence of foreign nuclei, pure vapors can be supercooled well beyond the point where they should spontaneously condense to the liquid phase. For water vapor in a carefully cleaned cloud chamber, supersaturations of approximately 4.2 are possible. Beyond this point, homogeneous nucleation occurs and the vapor spontaneously condenses dropwise. Considering the free energy of both the vapor and vapor drop-let systems Gibbs (Ref. 39) predicted the critical size of the condensation nuclei which would be required to initiate condensation for a particular supersaturation. This is given as

$$r_{cr} = \frac{2\sigma M}{\rho RT \ln S}$$

where

$r_{c,r}$ is the critical radius,

σ is the surface tension of the liquid phase,

M is the molecular weight,

ρ is the liquid density,

R is the universal gas constant,

T is the absolute temperature, and

S is the supersaturation

A plot of this critical droplet size versus super-saturation is presented in Fig. 35. The size range of dust particles normally present in the atmosphere is also noted. A typical size distribution for particulates commonly found over land is presented in Ref. 40. Over the size range from 0.1 to 10 μm the number of particles between any two radius values can be determined from

$$\Delta n \int_{r_1}^{r_2} = \frac{C'}{3 \ell_n 10} (r_1^{-3} - r_2^{-3})$$

where the value C' is dependent on local atmospheric conditions and can range from an average of 4 to as high as 400. Figure 36 (Ref. 40) presents a typical gradient of particle sizes as a function of altitude. A simplified view of heterogeneous condensation would indicate that dust particles as small as 0.05 μm in diameter would act as condensation nuclei as the relative humidity rose to 100 percent in the atmosphere. However, it has been experimentally determined that some particles below 0.05 μm in diameter are extremely effective as condensation nuclei. Ruedy (Ref. 41) states that, in general, dust particles one half the critical radius can be considered 100-percent effective in producing condensation. Silver iodide smokes with particles as small as 0.01 μm have been used as condensation nuclei and their effectiveness has been attributed to the crystalline structure of the AgI (Ref. 42). Some of the naturally occurring hygroscopic salts are also considered as especially effective condensation nuclei in the 0.01- to 0.1- μm range. Particular interest is expressed in this size range because, as is noted in Fig. 36, at altitudes between 0.5 and 5 km the number density of condensation particles above 0.1 μm in diameter decreases rapidly; therefore, the active particles among the Aitken nuclei become a more

significant factor in the condensation process. Also, the surface properties of this size of particle are more important in determining if they are effective as condensation nuclei, and therefore they would more likely be susceptible to contamination by hydrocarbon vapors.

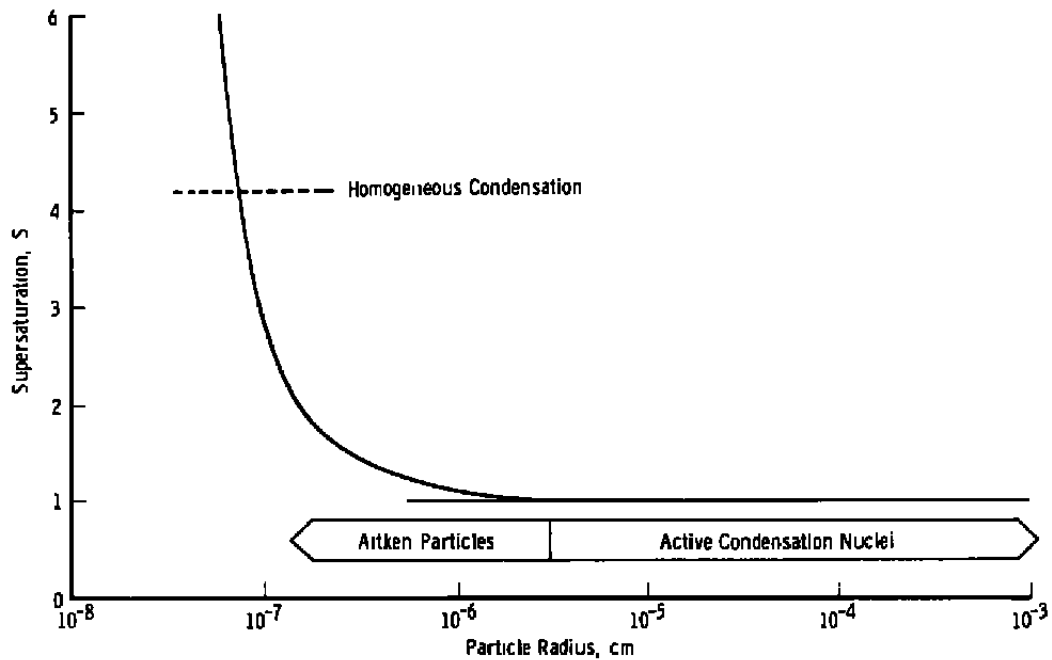


Figure 35. Critical supersaturation as a function of particle radius.

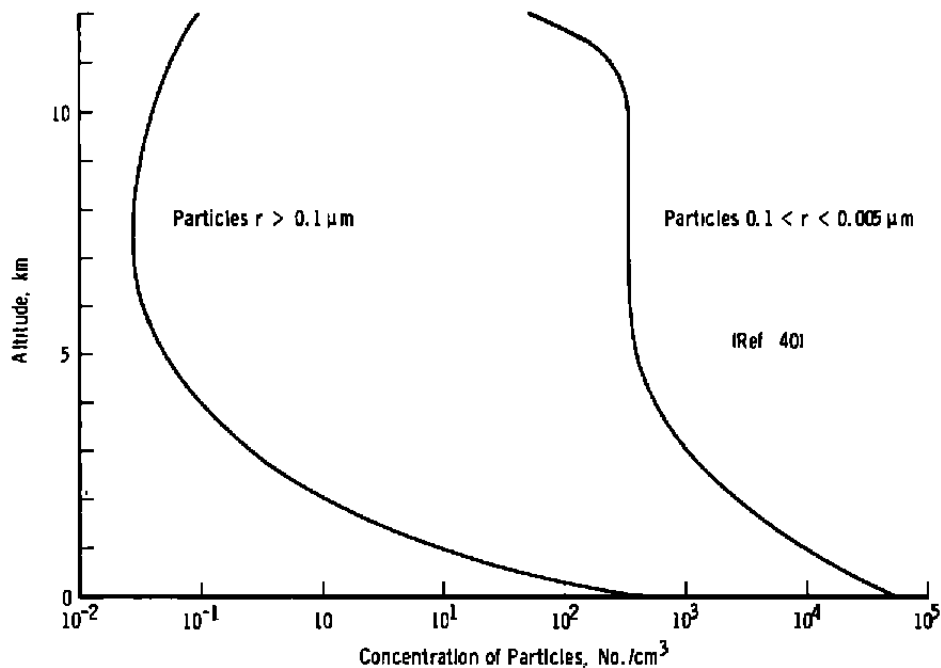


Figure 36. Concentration of condensation nuclei in atmosphere.

9.1 EXPERIMENTAL APPARATUS

The Wilson-type cloud chamber is shown schematically in Fig. 34. The glass cylinder which is partially filled with distilled water is fitted with a pneumatically operated piston and diaphragm. The air supply and the venting system to the piston are controlled by a series of electrically operated gate valves. These valves are in turn controlled by a timing sequencer which can be programmed to provide a series of expansions and compressions. The pressures in the test volume are monitored with a fast response transducer. The output from the transducer is also used along with a window comparator to provide feedback information to the timing sequencer to control the chamber pressure. The complete expansion chamber is housed in an insulated enclosure to maintain a constant temperature. Heaters located on the chamber base and a forced warm air circulation system in the upper part of the enclosure are thermostatically controlled to maintain a water temperature of $25 \pm 0.05^\circ\text{C}$ and a vertical temperature gradient of $1.0 \pm 0.05^\circ\text{C}$. Thermistors are used to monitor the temperatures and control the heater relays.

The air sample and the JP-4 vapors are introduced into and vented from the test volume via two ball valves located in the top plate. For complete air changes, a small vacuum pump is connected to the exhaust valve and the incoming air is drawn through a $0.4\text{-}\mu\text{m}$ filter. On those occasions when a specific quantity of room air was to be added to the test volume, the exhaust valve was opened and the piston operated to raise the water level the desired amount. The exhaust valve was then closed, the inlet valve opened, and the piston slowly lowered to draw the air sample into the test volume. JP-4 vapors are admitted using two techniques. For those tests requiring the more volatile fraction of JP-4 the cellulose support pad for the inlet filter was moistened with a measured volume, and the fluid and the vapors were drawn into the chamber along with the air sample. The pad was weighed before and after use to determine the quantity of the fuel remaining in the pad after the addition. Whole JP-4 vapors were admitted by opening the inlet ball valve and inserting a stainless steel tube fitted with a small heater. The sample was slowly introduced in the upper part of this tube from a calibrated syringe. The JP-4 was vaporized upon contact with the warm tube. A small purge of dry nitrogen was used to flush the residual vapors from the tube into the test chamber.

The data from these tests consist of visual observations of the test chamber and densitometer measurements from photographs taken of the

droplets in an illuminated volume. This volume is defined by a collimated light beam passing through the center of the test volume. The collimation slits are set 1.0 cm wide, although there is probably some distortion of the light beam as it passes through the curved glass walls of the chamber. Since in these experiments the absolute number density of droplets is not required, no further definition of the volume photographed was attempted. The camera was prefocused to the center of this volume.

9.2 EXPERIMENTAL PROCEDURE

The test chamber was cleared of all condensation nuclei by using the following procedure. The timing sequencer was programmed to slowly compress the volume to 900 mm, hold for five minutes, then produce a rapid expansion to 800 mm followed by a slow continuing expansion back to ambient pressure (745 mm). After holding at this condition for five minutes, the sequence was repeated. During these expansions, water vapor condenses on the active nuclei and the resulting droplets settle under gravitation into the liquid reservoir where the condensation particles are effectively trapped. Several cycles are necessary since during the settling process some of the smaller droplets in the upper part of the test volume evaporate before reaching the liquid surface.

After cleaning the nuclei from the test volume, a measured sample of room air was introduced using the technique of raising the piston as previously described. The timing sequence was then reprogrammed to produce the desired supersaturation and to trigger the camera and flash tube as the resulting droplets were produced.

After tests involving the addition of JP-4 vapor, the active volume was flushed with room air using the vacuum system and then readied for further tests by using the cleaning cycle. Periodically, the complete chamber was disassembled and cleaned to remove traces of JP-4 which accumulated on the glass walls of the chamber and the surface of the water in the reservoir.

9.3 RESULTS

The original intention was to introduce a small enough quantity of room air so that the number of droplets produced would be small enough to allow an individual droplet count for data analysis. However,

small samples resulting in droplet counts of 500 per ml or less were not repeatable enough to provide a baseline against which JP-4 contaminated samples could be compared.

With air samples of one liter, the initial droplet counts rose to an estimated 1000/ml. Comparisons of droplet densities were made by measuring the light transmitted through the negative with a commercial film densitometer. Only exposures on the same roll of film were compared in these tests since differences attributable to film development and processing not only shifted the absolute readings but also affected the normalized readings compared to a "standard" exposure taken as the first frame of each roll of film. The observations within each set of runs, however, were consistent.

The first series of runs consisted of photographing the droplets produced from one-liter samples of room air drawn through a 0.04- μ m filter. The supersaturation to trigger condensation was $S = 1.10$ and the same sample was subjected to four expansion cycles. The densitometer readings from this series are presented in Table 7a. As can be seen, the droplet density decreased significantly with each succeeding expansion due to the fallout and self-cleaning processing previously described. In expansions three and four, the densitometer is reading a background from light scattered from the glass walls and the surface of the liquid reservoir.

Table 7. Densitometer Readings
a. Densitometer Average Readings

Expansion No.	1	2	3	4
Sample No. 1	2.80	1.70	0.60	0.50
Sample No. 2	2.65	1.65	0.50	0.50
Sample No. 3	2.70	1.60	0.55	0.60
Sample No. 4	2.80	1.75	0.70	0.65
Average	2.73 ± 0.07	1.67 ± 0.07	0.58	0.56

The data presented in Table 7b are representative of runs made with JP-4 vapors added to the system. Again, the cleaning pattern follows that of the original control data and no significant differences are noted. Toward the end of this series of runs, it was noted that a visible film could be detected on the glass wall of the chamber. The

film was confined to a narrow band around the sidewall and clearly marked the high and low levels that the surface of the water attained during the compression and expansion cycles. This would indicate that the JP-4 vapors are being deposited on the surface of the water and then are migrating to the glass walls.

Table 7. Continued
b. Runs with JP-4 Vapor Added

Expansion No.	1	2	3	4
Sample (Air Only)	2.50	1.50	0.50	0.6
Sample 20 $\mu\ell$ JP-4	2.65	1.55	0.50	0.5
Sample 60 $\mu\ell$ JP-4	2.45	1.50	0.65	0.6
Sample 200 $\mu\ell$ JP-4	2.70	1.60	0.60	0.5

At this point, the system was disassembled and cleaned with detergent. After reassembly, a series of tests was made in which the most volatile fraction from a distillation series of JP-4 was used to "contaminate" the active volume (see Section 3.0 for properties of this fraction). The results of a typical run are recorded in Table 7c. The only difference that is possibly significant is that there would seem to be a few more drops persisting in the later expansions after approximately 1 ml of the No. 1 fraction had been added. Since the concentration of the vapor in this case is as high as would be expected in the immediate wake of an actual fuel dump, this slight effect would be considered insignificant as far as its impact on cloud formations.

Table 7. Concluded
c. Typical Run

Expansion No.	1	2	3	4
Sample (Air Only)	2.90	1.70	0.60	0.65
No. 1 Fraction 65 $\mu\ell$	2.95	1.85	0.70	0.60
No. 1 Fraction 418 $\mu\ell$	2.75	1.90	0.65	0.60
No. 1 Fraction 985 $\mu\ell$	2.80	1.95	0.95	0.60

The chamber was again disassembled and cleaned to remove a slight film appearing on the glass sidewalls. A final series of runs was made with an attempt to add a 1.0-ml sample of JP-4. The combination of an overheated addition tube and adding the sample too quickly resulted in a visible cloud of condensed JP-4 vapors entering the chamber. However, the cloud quickly dissipated, the ball valve was closed, and an expansion cycle was performed. The resulting supersaturation of $S = 1.10$ produced a dense fog which persisted for several minutes. Subsequent expansions eventually resulted in cleaning the chamber. This would indicate that JP-4 droplets themselves can act as effective condensation nuclei.

Further tests were made with similar additions of JP-4 droplets in which the initial cloud was observed during its lifetime along with the following cleaning expansions. In general, the droplets densities were much higher than in the previous tests and as a result the individual droplets were much smaller. It is felt that the greater number of cleaning cycles required to clean the chamber under these conditions can be attributed to the lower settling rates of the smaller droplets rather than any significant effects due to the JP-4.

9.4 DISCUSSION

The results obtained from these studies would indicate that the JP-4 vapors will be effectively scavenged and cleaned from the atmosphere by the natural process of condensation of water vapor and subsequent rainfall. The hydrocarbon vapors themselves do not appear to have any significant effect on the initiation of condensation of water vapor on atmospheric nuclei. In very high concentrations, they may tend to slow down the growth and decay rate of water droplets such as might be found in cloud formations. The major effect noted was the ability of small JP-4 droplets to act as condensation nuclei themselves. This would suggest that in the event of a fuel dump, under conditions where small droplets of JP-4 might survive and enter a parcel of humid air, these droplets may act as seed nuclei to initiate condensation. This could conceivably result in precipitation, thus concentrating a larger portion of the fuel than expected into a relatively small area at ground level.

10.0 SUMMARY OF RESULTS

A review of the literature indicates that very little work has been done which directly addresses the problem of dumping aircraft fuel into the atmosphere. In this work an attempt has been made to define some of the processes involved in the breakup of the initial liquid jet in order to better estimate the initial droplet-size distribution. Spray tests conducted at AEDC and observations of a high-altitude fuel dump have led to a suggested modification of the droplet-size distribution as reported in the literature (Ref. 4). This change would suggest that a larger percentage of the JP-4 is included in the smaller drop sizes than had been indicated.

Experiments were conducted to investigate the phenomenon of coalescence and its role in producing large droplets. The evidence indicates that large droplets are not produced by the coalescence of many small droplets. However, large droplets which are produced in the initial breakup process will grow slightly by collecting smaller droplets as they collide with them.

The theoretical work of Lowell (Refs. 31, 32, 33, and 34) was discovered early in the literature survey and his attempt to model the fallout process would seem to be a valid approach. Subsequent conversations with Dr. Lowell indicate that a computer code such as he developed could well profit from the subsequent advances in computer capabilities. The original computer program is no longer available and thus further work will be required to reproduce his code.

Some of the experiments in this program (e. g., determination of drag coefficients and evaporation properties) were conducted to help provide a firmer basis for some of the assumptions which must be made in such a computer program. Data from the experiments with free-falling JP-4 droplets have been presented in such a form as to be readily used to determine the terminal velocity of a particular size droplet. An alternate presentation is made in which knowing the terminal velocity the droplet size can be easily calculated. These data, plus information on evaporation rates of samples of JP-4 should provide basic inputs for predicting fallout rates and the possible survival of droplets to ground level.

Those properties of JP-4 such as density, vapor pressure, surface tension, etc., which are pertinent to the problem of atmospheric dumping have been collected from the various references and, in some cases,

these data have been supplemented with experimental values determined during these studies. Analysis of the vapors from freely falling droplets have shown that there is sufficient, internal circulation in the droplets to ensure that the more volatile species will evaporate first. This will result in fractionation of the JP-4 and thus leave the more volatile species at the higher altitudes. This information is of significance in considering the long term photochemical effects which may result from a fuel dump.

The cloud chamber studies indicate that the JP-4 vapors should have a negligible effect on the normal condensation processes in the atmosphere. The evidence suggests that condensation and rainfall will act as a scavenging process, thus removing some of the vapors. In this context, the only significant effect observed during these tests was the ability of small JP-4 droplets to act as condensation nuclei and thus conceivably serve as seeding material to initiate precipitation under some circumstances.

REFERENCES

1. Watkins, H. D. "Carriers Seek Alternatives to Turbojet Fuel Dumping." Aviation Week and Space Technology, November 2, 1970.
2. Stephens, E. R. "Chemistry of Atmospheric Oxidants." Journal of Air Pollution Control Association, Vol. 19, No. 3, March 1969, pp. 181-185.
3. Garrett, W. D. "Retardation of Water Drop Evaporation with Monomolecular Surface Films." Journal of the Atmospheric Sciences, Vol. 28, No. 5, July 1971, p. 816.
4. Cross, N. L. and Picknett, R. G. "Ground Contamination by Fuel Jettisoned from Aircraft." AGARD, CP-125, 1972.
5. Davidson, D. L. "Holographic Determination of the Droplet Size of a Simulated Defoamant Spray in a 400-Knot Airstream." AFATL-TR-70-47 (AD880066), May 1970.
6. Wasson, R. A., Darlington, C. R., and Billingsley, J. C. "Droplet Diameter and Size Distribution of JP-4 Fuel Injected into a Subsonic Airstream." AEDC-TR-74-117, April 1975.

7. Wigg, L. D. "The Effect of Scale on Fine Sprays Produced by Large Air Blast Atomizers." NGTE-R-236 (AD227044), July 1959.
8. Merrington, A. C. and Richardson, E. G. "The Breakup of Liquid Jets." The Proceedings of the Physical Society (London), Vol. 59, Part I, 1947.
9. Raleigh, Lord. "On the Instability of Jets." Proceedings of the London Mathematical Society, Vol. 10, 1878.
10. Nukiyama, S. and Tanasawa, Y. "Experiments on the Atomization of Liquids in an Air Stream, Reports 1 to 6 (5th Report-The Atomization Pattern of Liquid by Means of Air Stream), Summary Section, Translated from the Transactions of the Society of Mechanical Engineers, Japan, February 1940, Vol. 6, No. 22.
11. Castleman, R. A., Jr. "The Mechanism of the Atomization of Liquids." Bureau of Standards Journal of Research, Vol. 6, 1931, pp. 369-376.
12. Sauter, J. "Investigation of Atomization in Carburetors." NACA TM 518, 1929.
13. Lapple, C. E., Henry, J. P., Jr., and Blake, D. E. "Atomization - A Survey and Critique of the Literature." AD821314, Stanford Research Institute, Menlo Park, California, April 1967.
14. Ingebo, R. D. and Foster, H. H. "Drop-Size Distribution for Crosscurrent Breakup of Liquid Jets in Airstream." NACA TN-4087, October 1957.
15. Volynski, M. S. "On the Breakup of Droplets in an Air Stream." Akademiia nauk, SSSR, Doklady, Vol. 62, 1948, pp. 301-304.
16. Lane, W. R. "Shatter of Drops in Streams of Air." Industrial and Engineering Chemistry, Vol. 43, No. 6, 1951, pp. 1312-1317.
17. Schlichting, H. Boundary Layer Theory. McGraw-Hill, New York, 1955.
18. Gunn, R. and Kinzer, G. D. "The Terminal Velocity of Fall for Water Droplets in Stagnant Air." Journal of Meteorology, Vol. 6, August 1949.

19. Laws, J. O. "Measurement of the Fall Velocity of Water Drops and Rain Drops." Transactions of the American Geophysical Union, Vol. 22, Part III, 1940.
20. Johnston, R. K., Monita, C. M., and Kemper, W. A. "Physical and Chemical Properties of JP-4 Jet Fuel for 1970." AFAPL-TR-71-79, September 1971.
21. Maxwell, J. B. Data Book on Hydrocarbons. Van Nostrand, New York, 1950.
22. Barnett, H. C. and Hibbard, R. R. "Properties of Aircraft Fuels." NACA TN-3276, August 1956.
23. Taylor, H. S. and Taylor, H. A. Elementary Physical Chemistry. Second Edition, D. Van Nostrand Co., Inc., 1937, p. 172.
24. Hoerner, S. F. Fluid Dynamic Drag. Published by the Author, Midland Park, New Jersey, 1958.
25. Bailey, A. B. "Spheres Drag Coefficients at Subsonic Mach Numbers for a Broad Range of Reynolds Numbers," Journal of Fluid Dynamics, to be published.
26. Spilhaus, A. F. "Raindrops Size, Shape and Falling Speed." Journal of Meteorology, Vol. 5, 1948, pp. 108-110.
27. Magono, C. "On the Shape of Water Drops Falling in Stagnant Air." Journal of Meteorology, Vol. 11, 1954, pp. 77-79.
28. Hinze, J. O. "Forced Deformations of Viscous Liquid Globules." Applied Scientific Research, Series A, Vol. 1, 1947-48, pp. 263-272.
29. Frossling, N. "Über die Verdunstung Fallender Tropfen." Gerlands Beiträge für Geophysik, Vol. 52, 1938, pp. 170-216.
30. Ranz, W. E. and Marshall, W. R., Jr. "Evaporation from Drops, Part I." Chemical Engineering Progress, Vol. 48, 1952, pp. 141-146.
31. Lowell, Herman H. "Free Fall and Evaporation of n-Octane Droplets in the Atmosphere as Applied to the Jettisoning of Aviation Gasoline at Altitude." NACA RM E52L23a, 1953.
32. Lowell, Herman H. "Free Fall and Evaporation of JP-4 Jet Fuel Droplets in a Quiet Atmosphere." NASA TN D-33, September 1959.

33. Lowell, Herman H. "Dispersion of Jettisoned Jet Fuel by Atmospheric Turbulence, Evaporation, and Varying Rates of Fall of Fuel Droplets." NASA TN D-84, October 1959.
34. Lowell, Herman H. "Free Fall and Evaporation of JP-1 Jet Fuel Droplets in a Quiet Atmosphere." NASA TN D-199, March 1960.
35. Garner, F. H. and Skelland, A. H. P. "Liquid-Liquid Mixing as Affected by the Internal Circulation in Drops." Transactions of the Institution of Chemical Engineers, Vol. 29, 1951.
36. Schwartz, R. D. and Brasseaux, D. J. "Resolution of Complex Hydrocarbon Mixtures by Capillary Column Gas Liquid Chromatography." Analytical Chemistry, Vol. 35, No. 10, September 1963, pp. 1374-1382.
37. 1972 Annual Book of ASTM Standards. Part 17, American Society for Testing and Materials, Philadelphia, Pennsylvania 19103, 1972.
38. Richarz, F. "The Value of the Ratio of Specific Heats for a Mixture of Two Gases." Annalen der Physik, Vol. 19, 1906, p. 639.
39. Gibbs, J. W. The Collected Works of J. W. Gibbs. New York, Longmans, Green and Co., 1948.
40. Valley, Shea L., Editor. Handbook of Geophysics and Space Environments. Air Force Cambridge Research Laboratories. McGraw-Hill, New York, 1965.
41. Ruedy, R. "Transmission of Light by Water Drops 1 to 5 μ m in Diameter." Canadian Journal of Research, 1944, Section A22, p. 53.
42. Battan, L. J. Cloud Physics and Cloud Seeding. Doubleday Anchor, New York, 1962.

NOMENCLATURE

A	Surface area of droplets
C	Drag coefficient
C*	Evaporation coefficient

D	Diameter of jet
D*	Diffusion coefficient
d	Diameter of droplet
f	Fuel flow rate
g	Gravitational constant
k	Boltzmann's constant
M	Molecular weight
m	Mass of droplet
P	Pressure
R	Universal gas constant
Re	Reynolds number
Re'	Liquid film Reynolds number
r	Radius of droplet
S	Supersaturation
Sc	Schmidt number
T	Temperature
t	Time
V	Velocity
We	Weber number
We'	Inverse Weber number
γ	Ratio of specific heats
ϵ	Eccentricity
μ	Viscosity
ρ	Density
σ	Surface tension

SUBSCRIPTS

1	Initial condition
2	Final condition
cr	Critical
eff	Effective
g	Gas
l	Liquid
o	Equivalent
t	Terminal
v	Vapor
∞	Equilibrium value